
GENSTRAT: Toward a Science of Strategic Reasoning in Large Language Models

Vartan Shadarevian*
Princeton University

Kia Ghods
Princeton University

Alex Kenich
Google

Anany Kotawala
Princeton University

Abstract

Large language models (LLMs) are increasingly deployed as economic agents in marketplaces, auctions, and bidding settings. Anticipating their behavior in any specific deployment is hard. Existing strategic-reasoning benchmarks evaluate models on fixed canonical games. These benchmarks may saturate as the frontier improves, and they do not allow evaluators to generalize with confidence from benchmark performance to the varied and messy strategic environments that actual deployments involve. We introduce GENSTRAT, which uses procedurally generated strategic environments to address these challenges. Concretely, we generate a distribution of two-player zero-sum imperfect-information card games. The generator can draw fresh games on demand, allowing for evergreen evaluation and resistance to contamination. We pair the game distribution with a capability-profile methodology that decomposes model competence across six axes (state space, temporal depth, information sensitivity, opponent modeling, risk, and brittleness). We also introduce a jaggedness measure of within-distribution smoothness that detects when a model’s advantage jumps unpredictably between strategically similar games. We sample 50 benchmark games from a 2,000-game generated pool and evaluate nine frontier and open-weight LLMs in a head-to-head tournament with over 36,000 matches. Newer frontier-tier models score higher on average. Beyond that average, models with near-identical overall strength show qualitatively different capability profiles, and two of the top three leaderboard models (gpt-5 and claude) are noticeably more locally volatile than the third (gemini-3.1-pro), despite being close in overall strength. Together, the capability profile and the jaggedness measure give a deployment-relevant diagnostic that the overall ranking alone cannot provide.

1 Introduction

Frontier LLMs are increasingly placed in economic-agent roles in controlled experiments, including running small commerce operations [1] and participating in marketplace simulations [2], and they exhibit algorithmic-collusion behavior in LLM-based pricing studies [3]. As LLMs see more use in multi-agent strategic settings, how well a given model will actually perform once deployed has become hard to anticipate. AI model performance on canonical games does not transfer cleanly to the specific strategic environment in which a deployer would use the model.

Existing strategic-reasoning benchmarks evaluate LLMs on fixed canonical games and suites. Poker-based LLM evaluations and agents, including Leduc Hold’em and Texas Hold’em settings [4, 5], AvalonBench [6], Diplomacy [7], and broader game-theoretic and gameplay suites such as GTBench and GameBench [8, 9] all fall in this category. Two limits constrain their ability to serve as evaluations of deployment-relevant strategic capability. First, fixed game suites may saturate as the frontier improves, and the closer a benchmark’s contents are to canonical games, the harder it is to rule

*Corresponding author. vartan@princeton.edu

out corpus contamination from training data. Second, reducing a model’s strategic competence to performance on a small number of games limits the deployer’s ability to generalize from benchmark performance to novel strategic environments, where variation, real-world messiness, and shifts in information structure can profoundly affect optimal play.

We address both limits with GENSTRAT, a procedurally generated distribution of two-player zero-sum imperfect-information card games, which we call generalized betting games (GBGs). Procedural generation has proven productive for single-agent reinforcement learning generalization (ProcGen [10], MiniGrid [11]), but its potential for evaluating multi-agent strategic reasoning in LLMs has been less explored. Multi-agent settings exhibit an *amplification effect* that makes evaluation through procedural generation especially informative: small increases in the complexity of the underlying environment can produce substantial increases in the complexity of the resulting strategic problems agents face. Each game in our benchmark is played for chips, a numeric stake that accrues over the course of a match and determines the final payoff. Because the generator can draw freely from the same distribution at any time, the GENSTRAT benchmark cannot be saturated by training on the 50-game benchmark. Even if an evaluator that trains directly on those 50 games saturates that fixed subset, a held-out fresh draw from the same procedural distribution remains uncontaminated. We pair the distribution with a six-axis capability-profile decomposition (state space, temporal depth, information sensitivity, opponent modeling, risk, brittleness) so that a model’s performance is reported across strategic dimensions rather than through a single ranking. We also introduce a jaggedness measure that quantifies how sharply a model’s win-margin residuals fluctuate between similarly situated games.

We then run a 9-model tournament over more than 36,000 game matches (the merged tournament data contains 36,937 slot rows), including both open-weight and closed-source models. Larger, more recent, and reasoning-capable models score higher on average, with the leaderboard separating models across roughly three chips per game in a clean ordering. Models with near-identical overall strength show qualitatively different capability-profile shapes: `gemin-3.1-pro-preview` gains ground on the broadest set of axes, whereas `claude-sonnet-4-6-max` gains most of its ground on brittleness alone. The strongest tested model by mean win margin (`gpt-5-4-high`) is also among the most locally jagged (Section 8), whereas the second-strongest (`gemin-3.1-pro-preview`) is the smoothest among the top-tier models. A thinking-mode ablation, in which the same model plays anchor opponents at low and high reasoning effort across seven of the eight family-anchor combinations, finds that the chip-margin return to extra reasoning has positive point estimates of comparable magnitude across all four model families, with two of the four intervals excluding zero and the remaining two underpowered by sample size rather than null in expectation. The implication for deployment is that a model’s strategic capability is best understood as its full performance profile across different regions of the procedural game space, together with its level of local jaggedness.

2 Related work

Strategic games have played a longstanding role in AI research, including specific well-known cases like AlphaZero [12] on chess/Go, Libratus [13] and Pluribus [14] on poker, DeepNash [15] on Stratego, and CICERO [7] on Diplomacy. These evaluations often focused on isolated, specialized systems meant to play a single well-known game. They do not address generalization across novel strategic environments. More recently, efforts have been made to benchmark general-purpose LLMs against strategic games. For example, GTBench [8], GameBench [9], and AvalonBench [6] operate on fixed known games. Akata et al. [16] study LLMs in repeated games. Lorè and Heydari [17] disentangle game structure from contextual framing, Collins et al. [18] probe LLMs’ abilities to evaluate novel games, and Lin et al. [19] study LLMs on professional-poker-style tasks with agentic tool use. The Theory of Mind (ToM) literature is closely related. Strachan et al. [20] report human-level performance for some frontier models on classical false-belief tasks, while Ullman [21] shows that small task alterations can sharply reduce apparent ToM performance. The poker-ToM coding scheme of [22] is a closely related effort to read strategic reasoning from model traces.

Most closely related to our work, `gg-bench` [23] generates novel games via LLM authoring and evaluates LLMs on them by win rate against a self-play-trained reinforcement learning (RL) agent. GENSTRAT differs in four respects: (i) a parameterized rule generator (rather than LLM authoring), so the game distribution and its complexity are controlled by us directly rather than by an LLM’s design prior; (ii) game complexity scales arbitrarily through the same generator, letting the benchmark

track the model frontier without being rebuilt; (iii) we decompose performance along these axes of complexity and measure the jaggedness of model performance; (iv) we run a large-scale tournament to map the contours of model performance across these axes.

More broadly, measuring how foundation-model performance generalizes off the training-and-evaluation distribution has motivated a recent line of work on how people expect LLMs to generalize [24], on the implicit world model of generative models [25], and on inductive-bias probes for foundation models [26]. That work focuses on single-agent world modeling; our paper takes the same generalization concern to the multi-agent strategic setting that economic-agent deployment lands the model in.

Other work has examined procedural generation in other contexts as well, though in non-strategic settings. ProcGen [10], MiniGrid [11], and the broader procedural content generation literature [27] test single-agent RL generalization.

3 Generalized betting games and GENSTRAT

We define a generalized betting game (GBG) as a two-player zero-sum extensive-form game with imperfect information consisting of a deck, private hands, other card piles, structured phases, and conditions that gate branches of the game or otherwise control the occurrence of events. GBGs generalize games such as Kuhn poker [28] and Leduc poker [29] by adding features such as non-betting actions and rounds, alternative game tree and information structures, and different conditions for accessing branches of the game.

Structured phases determine how a game unfolds. They include betting phases, simultaneous-move phases, auction phases, and observation phases that give players access to signals or other information. For example, in variations with different levels of observability, the engine controls which observations are visible to each player.

The game-building engine randomizes the structural composition of a GBG, not just its surface parameters. The phase graph itself is sampled, so different draws yield structurally different game forms. Within that randomized structure, surface features such as ranks, suits, hand sizes, betting order, inclusion of other types of rounds (such as auction or simultaneous-move rounds), observation triggers, position criteria, showdown metrics, side-bet structures, and conditional-branch predicates are also drawn at random. Because randomized configurations can interact in non-trivial ways, the engine resolves the conditional structures that arise so that the resulting game remains coherent and playable. Further details on the modular construction are in Appendix A.

The complexity of generated games can be scaled by relaxing the generator caps used for the 50-game benchmark. The six axes introduced in Section 3.1 are Monte-Carlo-measured diagnostics rather than direct generator controls, but they are used at selection time to target coverage of specific regions of the axis space. Fresh evaluation games can be drawn from the same procedural distribution at any time, so training on the 50-game benchmark in Section 4 does not exhaust the procedural distribution. The generator can also produce games at higher complexity than the cap used for the 50-game benchmark, so the benchmark can scale with the model frontier. We ensure that every game is a deterministic function of its integer seed for reproducibility.

When games are generated, we apply multiple quality checks. A draw is only accepted if it passes three conditions based on Monte Carlo simulations involving random-playing agents. First, the average number of moves per player must be no more than ten. Second, every phase must fire in at least 5% of Monte Carlo episodes, with at most 30% of phases permitted to fall below that threshold before the game is rejected. Third, in games whose phase graph contains conditional branches, no more than 34% of those branches may remain dead across the Monte Carlo run. The Monte Carlo budget is 2,000 episodes per candidate game with the random agent that selects uniformly at random among legal actions at every decision node. To collect an accepted pool of 2,000 games, the procedural builder sampled 12,351 candidate seeds, of which roughly one in six passed the acceptance check to form the candidate pool from which the 50-game benchmark is then selected following the procedure in § 4.

3.1 Six complexity axes to characterize games

To better understand model performance variation across generated games and to ensure coverage of different notions of complexity, we compute six complexity ‘axes’ measuring the game along different dimensions, constructed from Monte Carlo simulation. Each axis captures a distinct strategic type of complexity that a player may face. Together they form the space we use for sampling games and measuring capability profiles (full formulas are provided in Appendix C).

- **State space.** The state space axis measures the general combinatorial complexity of the game. We approximate this as \log_{10} of the distinct observable information states observed by simulations of random-agent play. In this case, for example, small decks with fewer phases score low, whereas larger decks with more phases score high.
- **Temporal depth.** The temporal depth axis measures how strongly early decisions affect later payoffs. When early actions are inconsequential, a player can decide myopically. When they constrain or set up later phases, the player must plan forward. We measure this as the fraction of total payoff variance that is attributable to decisions taken early in the game, weighted by the number of remaining decisions that still lie ahead.
- **Information sensitivity.** The information sensitivity axis measures how strongly the best action depends on the player’s private information. When the optimal move changes with the private hand, the policy must condition on private state. In low-information-sensitivity games, a single near-best action works regardless. We measure this as the visit-weighted fraction of information-state buckets in which the argmax action depends on the player’s private information.
- **Opponent modeling.** The opponent modeling axis measures how much the best response shifts when the opponent’s policy changes. A game scores high when a player must adapt to opponent behavior, and low when the same action works against most opponents. We measure this as one minus the fraction of opponent policies (drawn from a Sobol low-discrepancy quasi-random sequence [30] over the probability simplex of mixed strategies, so opponent diversity is covered evenly with few samples) for which the single most-common best response remains optimal.
- **Risk.** The risk axis measures how much a game involves an expected-value-versus-downside tradeoff. A high-risk game has large upside and downside swings that force a tradeoff against worst-case payoff. A low-risk game has actions that are safe regardless of opponent play or chance. We measure this as the visit-weighted gap between the expected-value (EV) maximizing action and the downside-safest action at each decision, divided by the standard deviation of payoffs across decision instances so that the gap is dimensionless and comparable across games with different chip stakes.
- **Brittleness.** Brittleness measures the narrowness of the strategic margins. A brittle game has a payoff that changes sharply under small (3%) policy perturbations, so execution must be precise. We measure this as follows. The player’s best-response action is replaced with a uniformly random alternative at a set of decision contexts whose total visit probability sums to 3% of play. We then regress per-trial chip-margin change on whether the perturbation was applied at decision type dt , and report the ordinary least squares (OLS) slope as the brittleness contribution of dt .

Axis coverage. The pairwise Pearson correlation matrix across the 50 benchmark games (full matrix in Appendix D) shows that no two axes are too correlated: all pairwise $|r|$ are well below the values that would make joint analysis problematic. The strongest pairs are state-space \times information-sensitivity ($r=0.65$), state-space \times temporal-depth ($r=0.57$), and information-sensitivity \times opponent-modeling ($r=0.50$). Risk and brittleness are nearly independent of the rest ($|r|\leq 0.34$ with every other axis). The farthest-point sampling procedure (Section 4) promotes joint Euclidean coverage of the 6-axis cube subject to staying within the 2,000-game accepted pool. Marginal coverage on each axis follows as a consequence of the joint criterion rather than as a separate guarantee, and the realized 50 cover the full observed range on each axis without concentrating in any one corner. Variance inflation factors (VIF) are reported in Appendix D, all below the conservative VIF=5 rule of thumb (and well below the looser VIF=10 threshold).

4 Benchmark construction

From the 2,000-game accepted pool, we select 50 games via farthest-point sampling (FPS) in the six-axis embedding. Each axis is min-max normalized to $[0, 1]$, and FPS greedily picks the next game maximizing minimum Euclidean distance to the already-selected set, seeded with the centroid game. Figure 1 shows the 50 selected games in a scatter plot with state space and information sensitivity as axes. A scatter covering the full 2,000-game pool against the selected 50 is reported in Appendix E.

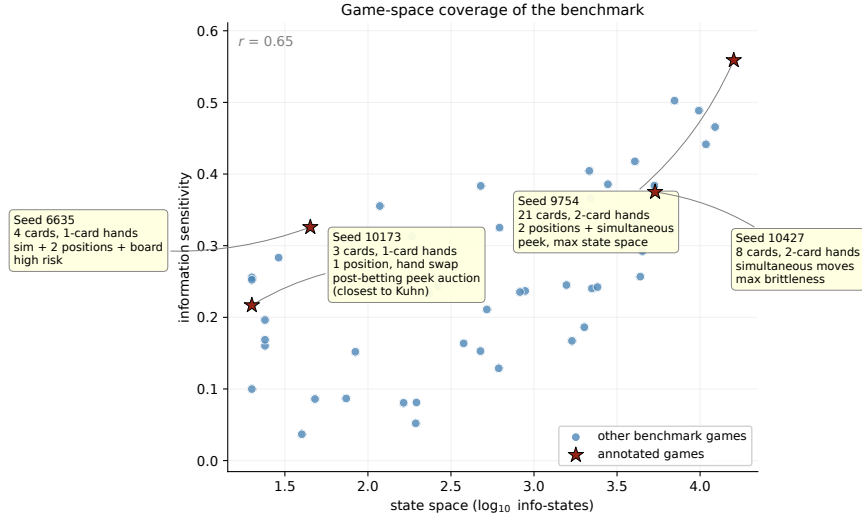


Figure 1: **The 50-game benchmark in two diagnostic axes (state space vs. information sensitivity).** Each point denotes a game, with stars marking the annotated games.

Per-axis coverage. Figure 2 plots the empirical distribution of each of the six axes across the 50 selected games. Dashed lines mark the per-axis 33rd and 67th percentiles, the cuts used for per-axis tertile splits elsewhere in the analysis. (The composite-complexity tertile split used in Appendix I is a separate construction based on a principal component of the per-model slope matrix, not on any single axis.) The state-space axis is reported in \log_{10} of the raw info-state count, and the underlying counts span roughly three orders of magnitude across the benchmark (from about 20 on Kuhn-like games to about 1.6×10^4 on the most complex), while the other five bounded axes have most of their mass concentrated toward the middle of the observed range with thinner tails on either side; we sample the full observed range on each axis but the bounded axes do not approach a flat distribution.

Three distributions appear in the pipeline and should be kept distinct. The first is the raw generator distribution, defined by the GBG sampling procedure of Section 3 before any quality gates apply. The second is the accepted pool, the subset of raw draws that pass the Monte Carlo acceptance filter described above, of which we collected 2,000 from 12,351 candidate seeds. The third is the 50-game evaluation benchmark obtained by farthest-point sampling within the accepted pool.

5 Tournament design

Models. Nine frontier and open-weight LLMs participate in the overall tournament: gpt-5-4-high, gemini-3.1-pro-preview, claude-sonnet-4-6-max, gemini-2.5-pro, gemma-4-31b-it, deepseek-v3.1-together, gemini-3.1-flash-lite-preview, qwen-3.5-together, and llama-3.3-70b-together. Per-model provider parameters are pinned to dated snapshots. Reasoning-capable models run with maximum thinking budget (`capability_tier=max_thinking`). Models without a thinking control run at provider defaults.

Pairing. A seat is one of the two player positions in a game. In each game there is a player seat ‘Alice’ and a player seat ‘Bob’. Most games are not symmetric across seats, so the seat a model occupies materially affects its payoff. For each (model 1, model 2, game) matchup we run 40 matches,

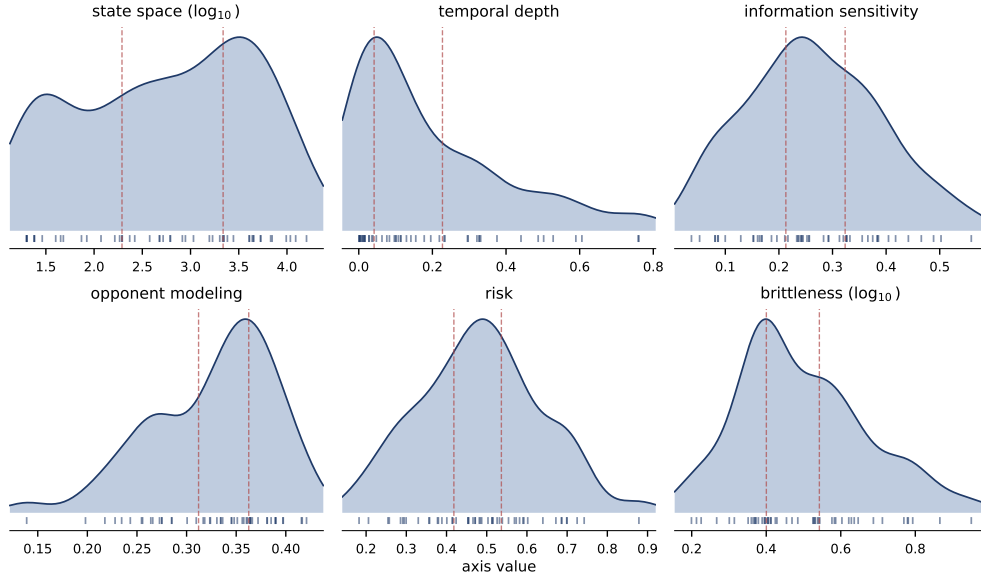


Figure 2: **Per-axis distributions of the 50 benchmark games.** Kernel-density estimates with tick-marked observations and tertile cuts (dashed). FPS achieves broad per-axis coverage on all six axes rather than concentrating on the two diagonal axes in Figure 1.

with each model occupying each seat in exactly 20 of them. A run groups two matches between the same two models, one with each seat assignment, sharing a deterministic `play_seed` derived from (game seed, run id, matchup) so that the same chance draws (dealing, shuffles, etc.) are played out under both seat assignments. A slot is one of those individual matches, i.e., a single (game seed, model 1, model 2, seat assignment, run id) match in the tournament. The merged tournament data is a table of slot rows.

Coverage. The tested models vary significantly in their per-token cost. To keep costs manageable, we vary which subset of possible matchups per game a model faces. We ensure that each model plays each game against at least two opponents. The merged tournament data contributes 36,937 rows (some matches hit time-out issues on multiple attempts and were discarded). Under the additive-strength specification, the paired-comparison estimator (Section 6) corrects for opponent-mix imbalance by fitting a single strength indicator $\hat{\alpha}_m$ for a model jointly across all matchups, so a model that plays a stronger or weaker mix of opponents than another is adjusted for in the strength comparison.

Prompt and parsing. Each model receives the auto-generated natural-language rulebook in its system prompt and a per-turn observation prompt composed from its visible history, current phase context, and legal action menu. Responses must terminate with a JSON object specifying the chosen action. A lenient parser recovers from minor format violations (stray whitespace, partial JSON). When both strict and lenient parsing fail, the engine selects a uniformly random legal action so play can continue. Per-model fallback rates are uniformly low (worst case 0.5% of moves) and are reported in Appendix F.

6 Overall results

Throughout this paper, payoffs are measured in chips, and all model-strength scores are reported in chips per game. For each model m we estimate a single strength score $\hat{\alpha}_m$ on a common chips-per-game scale.²

² $\hat{\alpha}_m$ is a continuous-margin analogue of a Bradley–Terry [31] paired-comparison rating. It uses the signed win margin in chips at the end of each match rather than the binary win/loss indicator that the standard Bradley–Terry model uses.

Estimator. We fit an additive paired-comparison model on match-level signed margins. Let y_s be the win margin (Alice chips minus Bob chips) at the end of match s , and let $i^{(s)}, j^{(s)}$ be the models seated as Alice and Bob in s . We fit

$$y_s = \alpha_{i^{(s)}} - \alpha_{j^{(s)}} + \varepsilon_s \quad \text{subject to} \quad \sum_m \alpha_m = 0.$$

The data identify only strength differences. An unconstrained fit is degenerate since adding a constant c to every α_m gives the same predictions. The sum-to-zero constraint anchors the level so the $\hat{\alpha}_m$ are uniquely identified, and consistent with the zero-sum structure of each game. Confidence intervals come from $B = 2,000$ paired-cluster bootstrap resamples, with clusters indexed by the four-tuple $c = (g, m_1, m_2, r)$, where g is a game seed, (m_1, m_2) is the unordered model pair, and r is the run id that uniquely identifies a paired play seed within that matchup. The two matches in a cluster (one for each seat assignment) share the same `play_seed`. B is the number of bootstrap resamples throughout this paper, fixed unless otherwise noted. The resulting $\hat{\alpha}_m$ is in chips/game.

Leaderboard. Table 1 reports overall strengths. GENSTRAT cleanly separates models across roughly three chips/game of range.

Table 1: **Overall leaderboard.**

Overall leaderboard — $\hat{\alpha}$ (chips/game)		
Model	$\hat{\alpha}$	95% CI
gpt-5-4-high	+0.85	[+0.74, +0.96]
gemini-3.1-pro-preview	+0.83	[+0.76, +0.91]
claude-sonnet-4-6-max	+0.64	[+0.52, +0.75]
gemini-2.5-pro	+0.37	[+0.29, +0.44]
gemma-4-31b-it	+0.25	[+0.18, +0.32]
deepseek-v3.1-together	+0.05	[-0.02, +0.13]
gemini-3.1-flash-lite-preview	-0.27	[-0.35, -0.20]
qwen-3.5-together	-0.35	[-0.44, -0.27]
llama-3.3-70b-together	-2.37	[-2.49, -2.23]

Paired-cluster bootstrap 95% CIs from $B=2,000$ resamples, fit on 36,937 tournament rows across the 50 benchmark games.

Pairwise margin matrix. The full matrix, consisting of pairwise differences in expected chips, is reported in Appendix J. Only 2 of the 72 off-diagonal entries showed a sign reversal from the expected chip margin based on the overall leaderboard.

Robustness checks. The overall ordering survives three perturbations of the data. Under **leave-one-game-out**, refitting $\hat{\alpha}$ with each of the 50 games dropped in turn preserves the order in 48 of 50 refits (mean Kendall $\tau=0.998$, min 0.944). Under **llama-excluded**, dropping the bottom outlier and refitting on the remaining eight models fully preserves relative order. Under **axis-space partition refits**, partitioning the 50 games into six clusters by their position in the 6-axis space and refitting $\hat{\alpha}$ inside each cluster yields per-cluster rankings that correlate with the overall at Spearman $\rho \geq 0.95$ in five of six clusters (the sixth is a two-game cluster with $\rho=0.87$). As an additional reference point, we ran an abstracted counterfactual regret minimization (CFR) [32] solver baseline in its CFR⁺ variant [33] on 5 tractable seeds against all 9 models (100 matches each); model performance against these 5 seeds correlates with the overall leaderboard at Spearman $\rho=0.95$ (Appendix K). Full tables are in Appendix H.

Bradley-Terry on win indicator. A win-only Bradley-Terry (BT) ranking on the same data gives a noticeably different ordering than $\hat{\alpha}$: small-margin frequent winners (e.g., `gemma-4-31b-it`) score higher under BT, while large-margin infrequent winners (e.g., `gpt-5-4-high`) score lower. The two estimators answer different questions. BT measures frequency of winning, while $\hat{\alpha}$ measures average

win margin. Since our models were expressly instructed to maximize expected chips rather than expected win probability, we report $\hat{\alpha}$ in the main text and treat the BT divergence as a complementary stress test rather than a contradiction. The full BT-vs- $\hat{\alpha}$ table is in Appendix H.

Composite-complexity tertile refits. We also collapse the six axes into a single per-game *composite-complexity* score. The construction proceeds in two steps. First, we compute the first principal component of the centered nine-by-six matrix of per-model axis-slopes, yielding a length-six weight vector with sign fixed so that the entries sum positive. Second, we project each game’s six-axis z -scored vector onto that weight vector to produce a single per-game scalar. The weights and construction details are in Appendix I. We then sort the 50 games on this score, split them into low, medium, and high composite-complexity tertiles, and refit $\hat{\alpha}$ within each tertile. Two findings emerge. First, the overall ranking is stable across tertiles: gpt-5-4-high and gemini-3.1-pro-preview occupy the top two ranks in every tertile, and llama-3.3-70b-together occupies the bottom rank in every tertile. Second, the gap between the top-three group and llama roughly doubles as composite complexity rises. The gap between the average top-three strength and llama’s strength is about 1.75 chips per game in the easiest tertile and about 4.5 chips per game in the hardest tertile. Mid-pack ordering reshuffles modestly in the easiest tertile, where the absolute gaps between mid-pack models are smallest. Per-tertile leaderboards are reported in Appendix I.

Per-game strength estimate $\hat{\alpha}_{m,g}$. The capability-profile and jaggedness analyses below also need a per-(model, game) strength, not just the overall $\hat{\alpha}_m$. We refit the additive paired-comparison model from the previous section separately on each game’s slot rows, with the sum-to-zero contrast applied across the models present on that game. The resulting $\hat{\alpha}_{m,g}$ is model m ’s win-margin strength on game g relative to the across-model mean of the nine models on g , and inherits the same opponent-mix correction the overall $\hat{\alpha}_m$ applies globally. A model that drew weaker opponents on game g is not credited with a higher per-game strength, because the opponent’s per-game $\hat{\alpha}$ on that game is also estimated on the same fit. Each of the $9 \times 50 = 450$ (model, game) pairs is identified on the merged tournament data. We use $\hat{\alpha}_{m,g}$ as a primitive throughout the rest of the paper.

To separate sources of variation in mean chip difference in (model 1, model 2, game) matchups, we decompose the variance of $\hat{\alpha}_{m,g}$ across the 450 (model, game) pairs. The variance of $\hat{\alpha}_{m,g}$ across the 450 pairs splits into a model main effect σ_M^2 , measuring how much $\hat{\alpha}_{m,g}$ varies from one model to another (i.e. the leaderboard signal), and a model \times game interaction σ_{MG}^2 , measuring how much a model’s strength on individual games deviates from its own average as the game changes. Formally, σ_M^2 is the variance across models of the per-model mean $\bar{\alpha}_m$, taken over the 50 games, and σ_{MG}^2 is the variance of the residuals $\hat{\alpha}_{m,g} - \bar{\alpha}_m - \bar{\alpha}_{.g} + \bar{\alpha}$ across the 450 pairs. The game main effect $\bar{\alpha}_{.g} - \bar{\alpha}$ is zero by construction because $\hat{\alpha}_{m,g}$ is sum-to-zero across models on every game (Section 6). Full definitions, including the within-cell bootstrap that propagates sampling noise into $\hat{\alpha}_{m,g}$, are in Appendix G. On the full nine-model dataset the leaderboard signal dominates but interaction remains substantial: the ratio σ_{MG}^2/σ_M^2 is 0.49, with a 95% paired-cluster bootstrap interval running from 0.36 to 0.65. If we exclude llama-3.3-70b, whose outlier position inflates the model main effect, the same ratio rises to 1.29 (bootstrap interval 0.64 to 2.19), so model \times game interaction is roughly comparable in magnitude to the model main effect among the remaining eight non-outlier models. A substantial fraction of the variance in per-(model, game) strength therefore reflects which model plays which game, and this is what the capability profiles in Section 7 decompose along the six axes. Full per-component table in Appendix G.

The aggregate leaderboard is a summary across 50 games, and the per-game ranking induced by $\hat{\alpha}_{m,g}$ need not agree with it. To test how far apart the two can be, we constructed a per-game rank-stability test that, for each game, compares the observed number of pairwise rank reversals against the leaderboard to the number expected under a noise-only null. The null fixes each true pairwise gap at the overall $\hat{\alpha}_{m_i} - \hat{\alpha}_{m_j}$ and treats the per-game ranking as a noisy draw from it, using the bootstrap-empirical pairwise standard error on the per-cell $\hat{\alpha}_{m_i,g} - \hat{\alpha}_{m_j,g}$ as the noise scale.³ We apply the Benjamini–Hochberg false discovery rate (BH-FDR) [34] procedure across the 50 games. Two patterns stand out. First, across the benchmark as a whole the per-game ranking departs from

³The per-game p -value is computed from a standard-normal approximation to the sum of pairwise reversal indicators, treating them as independent Bernoullis. The 36 pairwise reversals on a given game are not strictly independent because the per-game $\hat{\alpha}_{m,g}$ estimates share information through the joint per-game refit. The independence assumption is the standard construction for a sum of correlated Bernoulli indicators of this form.

the overall ranking by more than sampling noise alone would predict on a non-trivial fraction of games (15 of 50 at $q < 0.05$, 19 of 50 at $q < 0.10$). Here q denotes the Benjamini-Hochberg-adjusted p -value. A threshold of $q < 0.05$ bounds the expected proportion of false discoveries among rejected nulls at 5%. Second, this dispersion is concentrated almost entirely on the easiest games, with reversal significance falling sharply on more complex ones: 12 of the 16 lowest-composite-complexity games are reversal-significant at $q < 0.05$, but none of the 17 highest-complexity games are. On the hardest games the top models pull away by larger margins, and the per-game ranking tracks the overall order closely. We document the construction and per-game outputs of this rank-stability test in Appendix P.

7 Capability profiles

The overall ranking treats two models with similar mean win margin as equivalent even when their advantages come from distinct portions of game space. We want to separate overall model strength, already captured by $\hat{\alpha}$, from a model’s relative gains and losses in axis space, the profile shape that two models with similar overall rank can still differ on. Figure 3 reports that profile shape via a per-axis OLS fit of per-game strength $\hat{\alpha}_{m,g}$ on the six z -scored axes, in raw chips/game units.

The capability-profile regression. For each model m we fit, on the 50-game benchmark and with a per-model intercept:

$$\hat{\alpha}_{m,g} = \beta_{m,0} + \sum_{a=1}^6 \beta_{m,a} z_a(g) + \varepsilon_{m,g},$$

where $z_a(g)$ is the z -scored value of axis a on game g . $\hat{\beta}_{m,a}$ is the change in m ’s chip advantage or deficit versus the across-model mean per σ of axis a , controlling for the other five axes and for m ’s overall level (absorbed into the intercept). Because $\hat{\alpha}_{m,g}$ is sum-to-zero across the nine models on each game by construction (Section 6), the slopes automatically sum to zero across models on every axis: if one model gains ground with axis a , the rest of the model pool collectively falls behind. Confidence intervals come from $B = 500$ paired-cluster bootstrap resamples, with clusters indexed by the same (game seed, run id) pairing used in Section 6.

Per-model coefficients with bootstrap CIs and BH-corrected significance markers are reported in Appendix L; a level-restored companion plot (predicted per-game strength at each axis’s observed maximum, folding overall leaderboard level and profile shape back together) is in Appendix M.

Models with similar overall $\hat{\alpha}$ display structurally different profiles in how their chip advantage or deficit versus the rest of the model pool shifts with axis values. Brittleness is the single axis on which all three top-leaderboard models pull further ahead of the rest as the axis grows. `claude-sonnet-4-6-max` adds +0.27 chips/game per σ of brittleness (the largest single-axis pull-ahead in the table), `gpt-5-4-high` adds +0.23, and `gemini-3.1-pro-preview` adds +0.15, with all three slopes clearing BH at $q < 0.05$. `gemini-3.1-pro-preview` pulls ahead on the broadest set of axes among the top three, also gaining BH-significant ground on state space (+0.22) and opponent modeling (+0.13). `claude-sonnet-4-6-max`’s profile is the most concentrated of the three: brittleness dominates and the other five axes are flat after control. `gpt-5-4-high` pulls ahead on several axes (state space, information sensitivity, opponent modeling) but only the brittleness slope clears BH after correction.

At the other end, `llama-3.3-70b-together` falls further behind as information sensitivity (−0.40) and brittleness (−0.42) grow, both BH-significant. The other four axes are moderately negative but not BH-significant under the per-game-strength fit. `gemini-3.1-flash-lite-preview` has the most direction-splitting profile: it pulls ahead of peers on temporal depth (+0.18) and information sensitivity (+0.19) but falls further behind on state space (−0.30), opponent modeling (−0.14), and brittleness (−0.15), all five BH-significant. `qwen-3.5-together` loses BH-significant ground on risk (−0.19) and opponent modeling (−0.15); its temporal-depth and information-sensitivity slopes are moderately negative (−0.16 and −0.11) but do not survive BH correction, and the remaining two axes are near zero. The mid-pack `gemini-2.5-pro`, `gemma-4-31b-it`, and `deepseek-v3.1-together` are largely flat after axis controls, with their relative position not shifting much with any single axis. This is consistent with capability that scales evenly across axes rather than concentrating on any one.

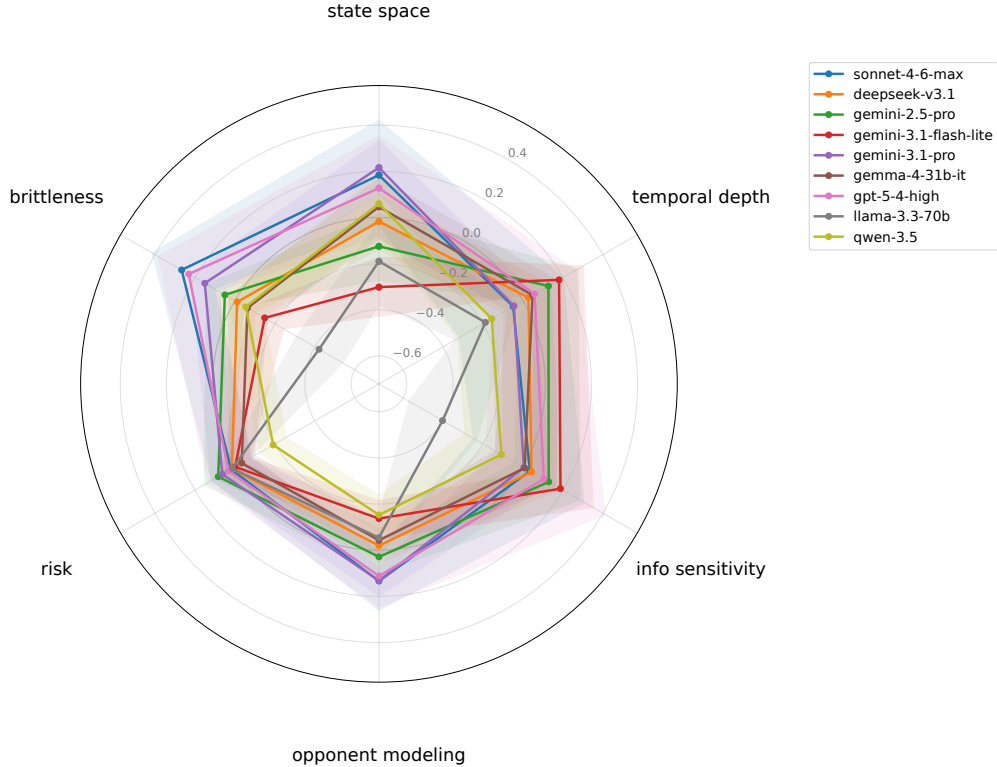


Figure 3: **Capability profile.** Per-model OLS slopes $\hat{\beta}_{m,a}$ of per-game strength $\hat{\alpha}_{m,g}$ on the six z -scored axes, fit with a per-model intercept on the 50 benchmark games. An outward slope indicates that the model’s chip lead over the across-model mean grows with that axis, while an inward slope indicates that the lead shrinks. Units are chips/game per σ of axis. Slopes sum to zero across the nine models on every axis by construction, since per-game $\hat{\alpha}_{m,g}$ is sum-to-zero across models on each game. Shaded bands are 95% paired-cluster bootstrap CIs ($B = 500$ resamples).

Robustness to rulebook-based confounds. Because the rulebooks our agents read are themselves auto-generated, the capability-profile slopes could in principle pick up rulebook-presentation effects rather than strategic structure. The most direct presentation confound is verbosity. The shortest rulebook in our 50-game benchmark is roughly 8,600 characters (approximately 2,000 tokens) and the longest is just under 39,000 characters (approximately 9,200 tokens), a span of roughly fivefold. We refit the per-model regression with the base-ten logarithm of the rulebook character count included as a regressor. The six axis slopes are stable to this control. No slope changes sign for any (model, axis) pair, and every pair that was BH-significant in Figure 3 remains significant. The length regressor absorbs only modest variance.

8 Local jaggedness

A capability profile reports each model’s average response to a single axis. Separately, a model’s win margin may vary smoothly between similar games or jump unpredictably between them. When the per-game win-margin surface is smooth, performance on one game extrapolates to nearby games in axis space. When the surface is jagged, considerable per-game volatility can be present beneath the overall $\hat{\alpha}_m$, and deployment outcomes on games that were not in the benchmark become harder to anticipate.

Construction of J_m . For each model m and game g we form the per-game deviation $\delta_{m,g} = \hat{\alpha}_{m,g} - \hat{\alpha}_m$, the model’s win-margin strength on game g minus its across-model strength. The deviation averages to approximately zero across the 50 games for each model, and exactly zero when $\hat{\alpha}_m$ coincides with the unweighted mean of $\hat{\alpha}_{m,g}$. It also inherits the opponent-mix correction that

$\hat{\alpha}_{m,g}$ already applies. We then normalize this deviation by the per-game stakes scale σ_g , the standard deviation of all signed match margins played on game g (an intrinsic property of the game rather than of any one model). The studentized deviation is

$$z_{m,g} = \frac{\hat{\alpha}_{m,g} - \hat{\alpha}_m}{\sigma_g}.$$

The denominator σ_g is a per-game empirical scale, computed from the realized match-margin distribution on game g , and is therefore not a property of the rulebook alone. It depends on the tested model pool, the schedule of matchups, and the retained slot rows. σ_g should be read as a common per-game denominator within this tournament rather than as a game invariant.⁴

To turn the $z_{m,g}$ surface into a per-model scalar, we average local axis-space dispersion using a K -nearest-neighbor (kNN) aggregator. For each game g , let $N_K(g)$ be its three nearest neighbors in the six-axis space, with each axis min-max-normalized to $[0, 1]$ before the Euclidean distance is taken. Write $\mathcal{N}(g) = \{g\} \cup N_K(g)$ for the four-game neighborhood of g (with $K = 3$), and $\bar{z}_{m,g} = \frac{1}{|\mathcal{N}(g)|} \sum_{g' \in \mathcal{N}(g)} z_{m,g'}$ for the model’s mean z -value on that neighborhood. We compute the population standard deviation of the neighborhood and average over all fifty benchmark games:

$$J_m = \frac{1}{|G|} \sum_{g \in G} \sqrt{\frac{1}{|\mathcal{N}(g)|} \sum_{g' \in \mathcal{N}(g)} (z_{m,g'} - \bar{z}_{m,g})^2}.$$

We compute 95% confidence intervals from a bias-corrected paired-cluster bootstrap. Robustness to the neighborhood size K and to alternative studentization choices is analyzed in Appendix N.

J_m as defined does not subtract the fitted capability-profile surface from $z_{m,g}$ before taking the local dispersion, so a smooth but steep trend across the six-axis space contributes to J_m alongside genuine local volatility.⁵

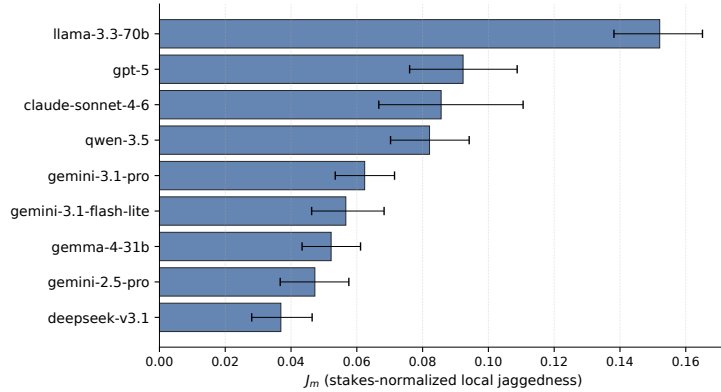


Figure 4: **Local jaggedness J_m , per model.** Bars sorted ascending, with horizontal whiskers showing bias-corrected paired-cluster bootstrap 95% confidence intervals ($B = 500$). Higher J_m means the stakes-normalized per-game performance surface swings more between axis-space-similar games.

Interpreting J_m . llama-3.3-70b-together is the most locally jagged model, with a central J_m of 0.152 and a 95% confidence interval that runs from 0.138 to 0.165. That lower bound exceeds the upper bound of every other model in the table, so the separation is substantive rather than an artifact of interval width. gpt-5-4-high and claude-sonnet-4-6-max are the next-most jagged, with central J_m values of 0.092 and 0.086 respectively, followed by qwen-3.5-together at 0.082. Their CIs overlap one another. At the smooth end of the table, deepseek-v3.1-together has the lowest central J_m (0.037), followed by gemini-2.5-pro (0.047), gemma-4-31b-it

⁴The dependence is less direct than for alternatives that divide explicitly by the model’s overall strength $|\hat{\alpha}_m|$ or by the typical opponent skill gap.

⁵ J_m also absorbs sampling noise in $\hat{\alpha}_{m,g}$ in addition to genuine per-game variation. The bias correction in the bootstrap removes a component of the inflation, but a fully sampling-noise-free analogue would require shrinking each $\hat{\alpha}_{m,g}$ toward a model-specific prior, an extension we leave to future work.

(0.052), `gemini-3.1-flash-lite-preview` (0.057), and `gemini-3.1-pro-preview` (0.062). One caveat is that the stakes-normalized measure does not condition on the model’s overall strength, so llama’s position at the top of the J_m table partly reflects the fact that its absolute chip-margin swings are larger across most games. We address this directly when pairing J_m with $\hat{\alpha}_m$ below.

Pairing J_m with $\hat{\alpha}_m$. Read together, J_m and $\hat{\alpha}_m$ recover four deployment-relevant regimes. High J_m paired with high $\hat{\alpha}_m$, as for `gpt-5-4-high` and `claude-sonnet-4-6-max`, describes top-tier strength with residual local volatility. These models are strong on average but have axis-space pockets of much higher or lower edge. They are also the most informative high- J_m cases, because their elevated jaggedness cannot be explained as a side-effect of weak play. Low J_m paired with high $\hat{\alpha}_m$, as for `gemini-3.1-pro-preview`, describes the smoothest top-tier strength regime, where performance on the fifty-game benchmark is the best guide to performance on neighboring draws. Low J_m paired with low or mid $\hat{\alpha}_m$, as for `deepseek-v3.1-together`, `gemini-2.5-pro`, and `gemma-4-31b-it`, describes consistently mid-pack performance with little axis-space surprise. The remaining regime is high J_m paired with low $\hat{\alpha}_m$, as for `llama-3.3-70b-together`, a weak model that also moves unpredictably across nearby games. The $(J_m, \hat{\alpha}_m)$ pair carries strictly more information than either alone, and two models with the same $\hat{\alpha}_m$ but different J_m should be deployed differently.

9 Reasoning ablation

We test whether extra thinking budget pays off uniformly across model families. We consider four families that have both a low-effort and a high-effort variant in the model registry: `gpt-5`, `claude-sonnet-4-6`, `gemini-3.1-pro`, and `gemini-2.5-pro`. For each family, we play both variants against two anchor opponents on identical shuffled decks. The anchors are `gemini-3.1-pro-preview`, a top-tier frontier model, and `gemma-4-31b-it`, a mid-pack open-weight model. We choose one anchor from each end of the leaderboard so that any thinking-budget effect we measure is averaged over both stronger and weaker opposition, rather than being tied to a single matchup. Every low-effort match has a high-effort sibling match in which the deal, the deck order, and the opponent are held constant, so any difference in win margin between the two siblings is attributable to the thinking budget rather than to chance variation in the cards. The estimand is the within-pair win-margin gain from going from low to high effort, $\Delta = \mathbb{E}[\text{win margin}_{\text{high}} - \text{win margin}_{\text{low}}]$. We fit $\hat{\Delta}$ on 620 such sibling pairs, spread across seven (family, anchor) cells, and report 95% confidence intervals from a cluster bootstrap on game seed.

Table 2: **Thinking ablation: paired- Δ win margin by family.** Families whose $\hat{\Delta}$ is significantly different from zero are starred.

Model family	$\hat{\Delta}$	95% CI	matches
<code>claude-sonnet-4-6</code>	+0.43	[-0.03, +0.97]	260
<code>gemini-2.5-pro</code>	+0.53	[-0.50, +1.50]	80
<code>gemini-3.1-pro*</code>	+0.44	[+0.24, +0.60]	50
<code>gpt-5*</code>	+0.21	[+0.02, +0.41]	230

* 95% CI excludes 0.

The four central estimates are positive and of comparable magnitude, ranging from +0.21 for `gpt-5` to +0.53 for `gemini-2.5-pro`. Two of the four intervals exclude zero, and the other two do not, but the difference between significant and non-significant rows is largely a difference in interval width rather than in the central effect. The non-significant rows are therefore better read as underpowered at the current sample size than as evidence of a null return to extra reasoning. We note, separately, that each provider implements the low-effort/high-effort dial differently. The `claude-sonnet-4-6` and `gpt-5` families expose an explicit reasoning-token budget. The Gemini families switch a discrete thinking mode on or off. The differences in match counts (50 to 260) reflect which models we could schedule paired siblings on.

10 Limitations and discussion

Data, methodology, and scope. Axis-conditional analyses at fifty games are directionally robust, but a larger benchmark would tighten the estimates further. Even with our farthest-point sampling, the state-space-related axes carry mechanical correlations with the other axes, so the six axes are complementary rather than fully orthogonal. Provider snapshots are pinned to dated model identifiers, so later snapshots are not guaranteed to reproduce the ordering. GENSTRAT covers two-player zero-sum imperfect-information English-language betting games. Cooperative, multi-player, non-betting, post-training, agentic-scaffold, and heuristic-baseline settings are left to future work.

All reported quantities, including the leaderboard, the capability profiles, and the jaggedness measures, are computed under a sum-to-zero contrast across the nine tested models and are therefore comparisons within the model pool. The CFR baseline on five tractable seeds is the only absolute reference point in our evaluation, and the remaining results should be read as relative rather than as a calibration of absolute strategic competence on the GBG distribution.

Broader impacts and deployment implications. Frontier LLMs are deployed as economic agents in marketplace, auction, and bidding settings (Section 1). The leaderboard ordering is stable across leave-one-game-out and composite-complexity tertile refits within the 50-game benchmark, so the relative ranking of models does not depend on any particular subset of games within the procedural distribution that the six axes span. We are more limited in our ability to evaluate strategic settings whose axis scores fall outside the range covered by the 50-game benchmark, or whose structural properties differ entirely from GBGs. Extending the benchmark to higher complexity caps and to non-GBG strategic families is left to future work.

Within the span the benchmark covers, the overall $\hat{\alpha}$ ranking on its own is not enough to guide deployment. A model’s capability profile on the axes that match the deployment, taken together with its local smoothness J_m on the region of game space the deployment is closest to, is the deployment-relevant summary. A model with high overall $\hat{\alpha}$ but a flat slope on information sensitivity may be a less suitable candidate than its leaderboard rank suggests for a bidding marketplace in which private-value revelation matters. Similarly, a model with high J_m may perform less reliably in a deployment whose game distribution lies near but not inside the benchmark.

11 Conclusion

GENSTRAT reframes strategic-reasoning evaluation around a procedurally generated game distribution and a six-axis decomposition of strategic complexity, so that capability profiles, jaggedness, and ablations can be read off the same evaluation. The generator scales as models improve and extends naturally to richer action primitives, larger state spaces, and multi-player settings.

Acknowledgements

We thank Peter Henderson, Zeyu Shen, and Vikram Kakaria for valuable discussions, assistance, and feedback that helped shape this work.

References

- [1] Anthropic. Project Vend: Can Claude run a small shop? (And why does that matter?). Anthropic Research, 2025.
- [2] Anthropic. Project Deal: our Claude-run marketplace experiment. Anthropic, 2026.
- [3] Sara Fish, Yannai A Gonczarowski, and Ran I Shorrer. Algorithmic Collusion by Large Language Models, 2024. arXiv:2404.00806v5, revised 2026.
- [4] Jiaxian Guo, Bo Yang, Paul Yoo, Bill Yuchen Lin, Yusuke Iwasawa, and Yutaka Matsuo. Suspicion Agent: Playing Imperfect Information Games with Theory of Mind Aware GPT-4. In *First Conference on Language Modeling (COLM)*, 2024.
- [5] Chenghao Huang, Yanbo Cao, Yinlong Wen, Tao Zhou, and Yanru Zhang. PokerGPT: An End-to-End Lightweight Solver for Multi-Player Texas Hold’em via Large Language Model, 2024. arXiv:2401.06781.

- [6] Jonathan Light, Min Cai, Sheng Shen, and Ziniu Hu. AvalonBench: Evaluating LLMs Playing the Game of Avalon, 2023. arXiv:2310.05036v3.
- [7] Meta Fundamental AI Research Diplomacy Team (FAIR), Anton Bakhtin, Noam Brown, Emily Dinan, Gabriele Farina, Colin Flaherty, Daniel Fried, Andrew Goff, Jonathan Gray, Hengyuan Hu, Athul Paul Jacob, Mojtaba Komeili, Karthik Konath, Minae Kwon, Adam Lerer, Mike Lewis, Alexander H. Miller, Sasha Mitts, Adithya Renduchintala, Stephen Roller, Dirk Rowe, Weiyan Shi, Joe Spisak, Alexander Wei, David Wu, Hugh Zhang, and Markus Zijlstra. Human-level play in the game of Diplomacy by combining language models with strategic reasoning. *Science*, 378(6624):1067–1074, 2022.
- [8] Jinhao Duan, Renming Zhang, James Diffenderfer, Bhavya Kailkhura, Lichao Sun, Elias Stengel-Eskin, Mohit Bansal, Tianlong Chen, and Kaidi Xu. GTBench: Uncovering the Strategic Reasoning Limitations of LLMs via Game-Theoretic Evaluations. In *Advances in Neural Information Processing Systems (NeurIPS)*, volume 37, pages 28219–28253, 2024.
- [9] Anthony Costarelli, Mat Allen, Roman Hauksson, Grace Sodunke, Suhas Hariharan, Carlson Cheng, Wenjie Li, Joshua Clymer, and Arjun Yadav. GameBench: Evaluating Strategic Reasoning Abilities of LLM Agents, 2024. arXiv:2406.06613v2.
- [10] Karl Cobbe, Christopher Hesse, Jacob Hilton, and John Schulman. Leveraging Procedural Generation to Benchmark Reinforcement Learning. In *International Conference on Machine Learning (ICML)*, volume 119 of *Proceedings of Machine Learning Research*, pages 2048–2056. PMLR, 2020.
- [11] Maxime Chevalier-Boisvert, Bolun Dai, Mark Towers, Rodrigo Perez-Vicente, Lucas Willems, Salem Lahlou, Suman Pal, Pablo Samuel Castro, and J K Terry. MiniGrid & Miniworld: Modular & Customizable Reinforcement Learning Environments for Goal-Oriented Tasks. In *Advances in Neural Information Processing Systems (NeurIPS) Datasets and Benchmarks Track*, volume 36, pages 73383–73394, 2023.
- [12] David Silver, Thomas Hubert, Julian Schrittwieser, Ioannis Antonoglou, Matthew Lai, Arthur Guez, Marc Lanctot, Laurent Sifre, Dharshan Kumaran, Thore Graepel, Timothy Lillicrap, Karen Simonyan, and Demis Hassabis. A general reinforcement learning algorithm that masters chess, shogi, and Go through self-play. *Science*, 362(6419):1140–1144, 2018.
- [13] Noam Brown and Tuomas Sandholm. Superhuman AI for heads-up no-limit poker: Libratus beats top professionals. *Science*, 359(6374):418–424, 2018.
- [14] Noam Brown and Tuomas Sandholm. Superhuman AI for multiplayer poker. *Science*, 365(6456):885–890, 2019.
- [15] Julien Perolat, Bart De Vylder, Daniel Hennes, Eugene Tarassov, Florian Strub, Vincent de Boer, Paul Muller, Jerome T. Connor, Neil Burch, Thomas Anthony, Stephen McAleer, Romuald Elie, Sarah H. Cen, Zhe Wang, Audrunas Gruslys, Aleksandra Malysheva, Mina Khan, Sherjil Ozair, Finbarr Timbers, Toby Pohlen, Tom Eccles, Mark Rowland, Marc Lanctot, Jean-Baptiste Lespiau, Bilal Piot, Shayegan Omidshafiei, Edward Lockhart, Laurent Sifre, Nathalie Beauguerlange, Remi Munos, David Silver, Satinder Singh, Demis Hassabis, and Karl Tuyls. Mastering the game of Stratego with model-free multiagent reinforcement learning. *Science*, 378(6623):990–996, 2022.
- [16] Elif Akata, Lion Schulz, Julian Coda-Forno, Seong Joon Oh, Matthias Bethge, and Eric Schulz. Playing repeated games with large language models. *Nature Human Behaviour*, 9(7):1380–1390, 2025.
- [17] Nunzio Lorè and Babak Heydari. Strategic behavior of large language models and the role of game structure versus contextual framing. *Scientific Reports*, 14(1):18490, 2024.
- [18] Katherine M. Collins, Cedegao E. Zhang, Graham Todd, Lance Ying, Mauricio Barba da Costa, Ryan Liu, Prafull Sharma, Adrian Weller, Ionatan Kuperwajs, Lionel Wong, Joshua B. Tenenbaum, and Thomas L. Griffiths. Evaluating Language Models’ Evaluations of Games. In *International Conference on Learning Representations (ICLR)*, 2026.
- [19] Minhua Lin, Enyan Dai, Hui Liu, Xianfeng Tang, Yuliang Yan, Zhenwei Dai, Jingying Zeng, Zhiwei Zhang, Fali Wang, Hongcheng Gao, Chen Luo, Xiang Zhang, Qi He, and Suhang Wang. How Far Are LLMs from Professional Poker Players? Revisiting Game-Theoretic Reasoning with Agentic Tool Use. In *International Conference on Learning Representations (ICLR)*, 2026.
- [20] James W. A. Strachan, Dalila Albergo, Giulia Borghini, Oriana Pansardi, Eugenio Scaliti, Saurabh Gupta, Krati Saxena, Alessandro Rufo, Stefano Panzeri, Guido Manzi, Michael S. A. Graziano, and Cristina Becchio. Testing theory of mind in large language models and humans. *Nature Human Behaviour*, 8(7):1285–1295, 2024.
- [21] Tomer Ullman. Large Language Models Fail on Trivial Alterations to Theory-of-Mind Tasks, 2023. arXiv:2302.08399v5.
- [22] Hsieh-Ting Lin and Tsung-Yu Hou. Readable Minds: Emergent Theory-of-Mind-Like Behavior in LLM Poker Agents, 2026. arXiv:2604.04157.
- [23] Vivek Verma, David Huang, William Chen, Dan Klein, and Nicholas Tomlin. Measuring General Intelligence with Generated Games, 2025. arXiv:2505.07215.

- [24] Keyon Vafa, Ashesh Rambachan, and Sendhil Mullainathan. Do Large Language Models Perform the Way People Expect? Measuring the Human Generalization Function. In *International Conference on Machine Learning (ICML)*, volume 235 of *Proceedings of Machine Learning Research*, pages 48919–48937. PMLR, 2024.
- [25] Keyon Vafa, Justin Y. Chen, Ashesh Rambachan, Jon Kleinberg, and Sendhil Mullainathan. Evaluating the World Model Implicit in a Generative Model. In *Advances in Neural Information Processing Systems (NeurIPS)*, volume 37, pages 26941–26975, 2024.
- [26] Keyon Vafa, Peter G. Chang, Ashesh Rambachan, and Sendhil Mullainathan. What Has a Foundation Model Found? Using Inductive Bias to Probe for World Models. In *International Conference on Machine Learning (ICML)*, 2025.
- [27] Noor Shaker, Julian Togelius, and Mark J Nelson. *Procedural Content Generation in Games*. Springer, 2016.
- [28] Harold W. Kuhn. A simplified two-person poker. In H. W. Kuhn and A. W. Tucker, editors, *Contributions to the Theory of Games, Vol. I*, number 24 in *Annals of Mathematics Studies*, pages 97–103. Princeton University Press, 1950.
- [29] Finnegan Southey, Michael Bowling, Bryce Larson, Carmelo Piccione, Neil Burch, Darse Billings, and Chris Rayner. Bayes’ Bluff: Opponent Modelling in Poker. In *Proceedings of the Twenty-First Conference on Uncertainty in Artificial Intelligence (UAI)*, pages 550–558, 2005.
- [30] I. M. Sobol’. On the distribution of points in a cube and the approximate evaluation of integrals. *USSR Computational Mathematics and Mathematical Physics*, 7(4):86–112, 1967.
- [31] Ralph Allan Bradley and Milton E. Terry. Rank Analysis of Incomplete Block Designs: I. The Method of Paired Comparisons. *Biometrika*, 39(3/4):324–345, 1952.
- [32] Martin Zinkevich, Michael Johanson, Michael Bowling, and Carmelo Piccione. Regret minimization in games with incomplete information. In *Advances in Neural Information Processing Systems (NeurIPS)*, volume 20, pages 1729–1736, 2007.
- [33] Oskari Tammelin. Solving Large Imperfect Information Games Using CFR⁺, 2014. arXiv:1407.5042.
- [34] Yoav Benjamini and Yosef Hochberg. Controlling the False Discovery Rate: A Practical and Powerful Approach to Multiple Testing. *Journal of the Royal Statistical Society. Series B (Methodological)*, 57(1):289–300, 1995.

A Modular game design

Each GBG is assembled from modular components composed by the parameterized GBG builder:

- **Core layer.** GameState (players, variables, piles), Rulebook (phase graph), Phase (ordered action lists).
- **Action subclasses.** Every game operation is a typed Action subclass (Deal, ChipTransfer, Shuffle, PeekAtHand, SwapWithOpponent, StealCardMove, Wager, ScoreAdjustment, ...), enabling structured logging and analysis.
- **Phase blocks.** Reusable make_action_round(), make_observation_round(), make_simultaneous_round(), and make_position_assignment_round() compose phases from parameterized templates.
- **Phase graph.** Conditional transitions between phases gated by chip counts, card comparisons, and round counters enable nonlinear game flow (branches, bounded loops, conditional sub-phases).
- **Complexity dial.** A single parameter $c \in [0, 1]$ modulates the draw probabilities for more complex structural and surface features, so increasing c smoothly shifts the distribution from Kuhn-like simplicity toward multi-phase complexity.
- **Deterministic reconstruction.** $G = \text{reconstruct}(s)$ exactly reproduces any game from its seed s given the builder version hash.

Natural-language rulebooks (Appendix B) are auto-generated from the phase graph and served as LLM system prompts. The rendering preserves all conditional structure, visibility rules, and chip-transfer semantics.

B Sample game rulebook

Relative to the 50 benchmark games, seed 4643 scores high on state-space (90th percentile), temporal-depth (98th), and risk (94th); low-to-mid on information-sensitivity (32nd) and opponent-modeling (30th); and mid-high on brittleness (72nd). The rulebook below is the verbatim system prompt the LLM agents receive at the start of play. It is constructed deterministically from the phase graph.

```
## Overview
**Players:** Alice, Bob
**Player order:** Player 1 = Alice (acts first in betting), Player 2 = Bob.
**Deck:** 3 cards (J, Q, K of hearts)
**Starting chips:** 10 each (visible to all). Chips move between players' stacks and the pot; the total of all chips (stacks plus pot) is conserved across the game.
**Pot:** starts at 0
**General rules:**
- **Information:** The number of cards remaining in the Deck is public information. Hand sizes are private. Players do not know how many cards opponents hold unless revealed by an action. If the Deck is empty when a draw action occurs, no cards are drawn and the action has no effect. Public draws emit a public skipped-draw notice; private draws emit that notice only to the drawing player - but per the inferability principle, the Deck-size change from any successful draw is publicly visible.
- **Legal actions:** Players may choose any listed option. If its preconditions are unmet (empty hand), the action has no effect.
- **Resolution:** In any multi-step effect, each step resolves in order; if one step's precondition is unmet, that step is skipped and later steps still resolve.
- **Game end:** If the game ends during any phase, all remaining phases are skipped.
- **Costs & pot:** Costs are paid to the pot before the effect resolves, unless otherwise specified. When an action lists a cost: if the player cannot afford the stated cost at the moment they select it, the action is not offered as an option. If the cost is probabilistic (e.g. a 50% chance of paying 1 chip), the player commits to the action first and the cost is resolved afterwards; if they cannot afford the resolved cost, the action is skipped and their choice slot is consumed (they do not get to pick again).
- **Showdown & misc.:** There is no hand size limit; hands grow and shrink freely via draws. Unless stated otherwise, all random selections are uniform. At Showdown, each player's hand is revealed as of the moment the Showdown phase begins, including any cards swapped, drawn, or stolen during earlier phases.
## Visibility
- **Hands:** Each player's cards are private to that player. Opponents cannot see hand contents unless explicitly revealed.
- **Actions:** All player actions (bets, checks, folds) and their effects are publicly announced unless stated otherwise. Actions marked as private are executed silently.
- **Inferability:** "Private" hides *which branch fired, what card was drawn/peeked, or who chose what* - not the observable side-effects. Deck sizes, pot totals, chip stacks, and position holdings are always public and reconcile at settlement. If one private branch would change a public number (e.g. shrink the Deck by 1) and another would not, the opponent can infer which branch ran from that number. Treat the privacy label as concealing the *identity/choice*, not the *occurrence*.
- **Condition checks:** Checks marked "(public)" are announced to all players when evaluated.
- **Hidden information:** All hidden information is tracked and enforced; players are told only what the rules specify.

## Sequence of Play
1. **Setup:** shuffle deck, deal cards
2. **Ante Phase:** each player antes into the pot
3. **Betting Phase:** players may bet, check, fold, or call
4. **Post-Betting Phase**
5. **Showdown:** reveal hands and settle the pot

## Phase Details

### Setup
- Shuffle the Deck.
- Deal 1 card face-down to each player (Alice, Bob) (or as many as remain if the deck is short). Each player sees only their own cards.

### Ante Phase
- Alice antes 2 chips (moved from Alice's chip stack into the pot).
- Bob antes 2 chips (moved from Bob's chip stack into the pot).

### Betting Phase
- Betting proceeds for up to 2 rounds.
- Each round, Betting Round is played. This continues until a player has 2 or fewer chips, the round cap (2) has been reached, or the game has ended.

#### Sub-phase: Betting Round *(called from Betting Phase)*
- <bet round> starts at 0 and increases by 1 after each round.
- If <bet round> is greater than 0 and the game is still in progress (public): Perform **Inter-Round Draw (All Players, inter-round event 1)** steps, then continue.
- If <bet round> is greater than 0 and the game is still in progress (public): Perform **Simultaneous Round (inter-round)** steps (both players participate per this sub-phase's own rules), then continue.
- If <bet round> is equal to 0 (public):
  - If Alice has chips remaining and Bob has chips remaining (public):
    Round 1: variable betting, wager any amount from 1 chip up to your remaining stack.
    Then, perform **Variable Betting Round (Round 1)** steps, then continue.
  - Otherwise:
    Round 1: variable betting unaffordable, falling back to fixed 1-chip betting for this round.
    Then, Alice picks one of: bet or check. (choice is announced to all players)
    - If Alice chooses 'check' (public): Perform **Bob: Bet or Check (Round 1, Fallback)** steps, then continue.
    - Otherwise, if Alice chooses 'bet':
      Alice bets 1 chip (moved from Alice's chip stack into the pot).
      Then, perform **Bob: Fold or Call (Round 1, Fallback)** steps, then continue.
```

```

- Otherwise:
  Round 2: fixed betting, each bet or call is 1 chip.
  Then, Alice picks one of: bet or check. (choice is announced to all players)
  - If Alice chooses 'check' (public): Perform **Bob: Bet or Check (Round 2)** steps, then continue.
  - Otherwise, if Alice chooses 'bet':
    Alice bets 1 chip (moved from Alice's chip stack into the pot).
    Then, perform **Bob: Fold or Call (Round 2)** steps, then continue.
*(Play returns to **Betting Phase**.)*

#### Sub-phase: Inter-Round Draw (All Players, inter-round event 1) *(called from Betting Round)*
- If the Deck has at least 2 cards (public): Inter-round draw: each player draws 1 card from the Deck (private).
  - Otherwise: Inter-round draw: the Deck has fewer than 2 cards remaining; the both-players draw is skipped.
*(Play returns to **Betting Round**.)*

#### Sub-phase: Simultaneous Round (inter-round) *(called from Betting Round)*
- All players choose simultaneously and in secret. No player knows the others' choices until all are locked in. Once
all choices are submitted, each player's choice is publicly revealed, then the combined outcome is resolved and
announced publicly. If a player fails to choose, a uniformly random option is selected for them.
- Alice chooses one of the following options: Hold or Parry.
- Bob chooses one of the following options: Hold or Parry.
- Outcomes based on choices:
  - If Alice chooses 'Hold' AND Bob chooses 'Parry':
    - If Bob's highest-ranked card has a higher rank than Alice's highest-ranked card: Alice pays 3 chips to Bob.
    If Alice has fewer than 3 chips, only the available amount is transferred.
  - Otherwise: Bob pays 1 chip to Alice. If Bob has fewer than 1 chip, only the available amount is transferred.
    *(The branch condition is evaluated privately; which branch fires is not announced directly.)*
    *(Note: different branches produce different observable chip effects; the branch taken may be partially
inferable from chip changes.)*
  - If Alice chooses 'Parry' AND Bob chooses 'Hold': Bob pays 1 chip to Alice. If Bob has fewer than 1 chip, only the
available amount is transferred.
  - If Alice chooses 'Parry' AND Bob chooses 'Parry': No effect.
  - If Alice chooses 'Hold' AND Bob chooses 'Hold':
    - If Bob holds at least one card of rank K or J:
      Alice peeks at 1 card in Bob's hand (selected uniformly at random). The card remains in Bob's hand. The
peek is private: only Alice sees the card. If Bob's hand is empty, Alice is informed that it is empty.
      Then, Alice pays 1 chip to Bob. If Alice has fewer than 1 chip, only the available amount is transferred.
    - Otherwise:
      Alice peeks at 1 card in Bob's hand (selected uniformly at random). The card remains in Bob's hand. The
peek is private: only Alice sees the card. If Bob's hand is empty, Alice is informed that it is empty.
      Then, Bob pays 1 chip to Alice. If Bob has fewer than 1 chip, only the available amount is transferred.
      *(The branch condition is evaluated privately; which branch fires is not announced directly.)*
      *(Note: different branches produce different observable chip effects; the branch taken may be partially
inferable from chip changes.)*
*(Play returns to **Betting Round**.)*

#### Sub-phase: Bob: Fold or Call (Round 2) *(called from Betting Round)*
- Bob picks one of: fold or call. (choice is announced to all players)
  - If Bob chooses 'call' (public): Bob bets 1 chip (moved from Bob's chip stack into the pot).
  - Otherwise, if Bob chooses 'fold':
    The entire pot is given to Alice.
    Then, the game ends: Alice wins after Bob folds.

#### Sub-phase: Bob: Bet or Check (Round 2) *(called from Betting Round)*
- Bob picks one of: bet or check. (choice is announced to all players)
  - If Bob chooses 'check' (public): No action.
  - Otherwise, if Bob chooses 'bet':
    Bob bets 1 chip (moved from Bob's chip stack into the pot).
    Then, perform **Alice: Fold or Call (responding, Round 2)** steps, then continue.
*(Play returns to **Betting Round**.)*

#### Sub-phase: Alice: Fold or Call (responding, Round 2) *(called from Bob: Bet or Check (Round 2))*
- Alice picks one of: fold or call. (choice is announced to all players)
  - If Alice chooses 'call' (public): Alice bets 1 chip (moved from Alice's chip stack into the pot).
  - Otherwise, if Alice chooses 'fold':
    The entire pot is given to Bob.
    Then, the game ends: Bob wins after Alice folds.

#### Sub-phase: Bob: Fold or Call (Round 1, Fallback) *(called from Betting Round)*
- Bob picks one of: fold or call. (choice is announced to all players)
  - If Bob chooses 'call' (public): Bob bets 1 chip (moved from Bob's chip stack into the pot).
  - Otherwise, if Bob chooses 'fold':
    The entire pot is given to Alice.
    Then, the game ends: Alice wins after Bob folds.

#### Sub-phase: Bob: Bet or Check (Round 1, Fallback) *(called from Betting Round)*
- Bob picks one of: bet or check. (choice is announced to all players)
  - If Bob chooses 'check' (public): No action.
  - Otherwise, if Bob chooses 'bet':
    Bob bets 1 chip (moved from Bob's chip stack into the pot).
    Then, perform **Alice: Fold or Call (responding, Round 1, Fallback)** steps, then continue.
*(Play returns to **Betting Round**.)*

#### Sub-phase: Alice: Fold or Call (responding, Round 1, Fallback) *(called from Bob: Bet or Check (Round 1,
Fallback))*
- Alice picks one of: fold or call. (choice is announced to all players)
  - If Alice chooses 'call' (public): Alice bets 1 chip (moved from Alice's chip stack into the pot).
  - Otherwise, if Alice chooses 'fold':
    The entire pot is given to Bob.
    Then, the game ends: Bob wins after Alice folds.

```

```

#### Sub-phase: Variable Betting Round (Round 1) *(called from Betting Round)*
- Alice and Bob may each bet any whole number of chips (minimum 1). When a player bets, their chosen amount is transferred from their chip stack into the pot immediately. When a player calls, their matched amount is transferred to the pot; if they cannot match the full bet, they go all-in with their remaining chips and the excess from the original bettor is returned to that bettor. If both players check in sequence, the round ends with no additional chips moving.
- Alice picks one of: bet or check. (choice is announced to all players)
  - If Alice chooses 'check' (public): Perform **Bob: Bet or Check (Round 1)** steps, then continue.
  - Otherwise, if Alice chooses 'bet':
    Alice chooses a wager amount (minimum 1 chip, up to Alice's current chip count). When Alice commits the chosen amount, it is transferred from Alice's chip stack into the pot via the normal public chip announcement. If the submitted amount exceeds the legal maximum, the bid is clamped to the maximum (all-in or declared cap). If the submitted amount is malformed or below the minimum, the engine substitutes a uniform-random legal amount. In either case the submitting player is notified privately and play continues with the resolved amount.
    Then, perform **Bob: Fold or Call (Round 1)** steps, then continue.
*(Play returns to **Betting Round**.)*

#### Sub-phase: Bob: Fold or Call (Round 1) *(called from Variable Betting Round (Round 1))*
- Bob picks one of: fold or call. (choice is announced to all players)
  - If Bob chooses 'call' (public): Bob matches the bet. If they cannot match the full amount, they go all-in and only the matched portion from each player remains in the pot.
  - Otherwise, if Bob chooses 'fold':
    The entire pot is given to Alice.
    Then, the game ends: Alice wins after Bob folds.

#### Sub-phase: Bob: Bet or Check (Round 1) *(called from Variable Betting Round (Round 1))*
- Bob picks one of: bet or check. (choice is announced to all players)
  - If Bob chooses 'check' (public): No action.
  - Otherwise, if Bob chooses 'bet':
    Bob chooses a wager amount (minimum 1 chip, up to Bob's current chip count). When Bob commits the chosen amount, it is transferred from Bob's chip stack into the pot via the normal public chip announcement. If the submitted amount exceeds the legal maximum, the bid is clamped to the maximum (all-in or declared cap). If the submitted amount is malformed or below the minimum, the engine substitutes a uniform-random legal amount. In either case the submitting player is notified privately and play continues with the resolved amount.
    Then, perform **Alice: Fold or Call (responding, Round 1)** steps, then continue.
*(Play returns to **Variable Betting Round (Round 1)**.)*

#### Sub-phase: Alice: Fold or Call (responding, Round 1) *(called from Bob: Bet or Check (Round 1))*
- Alice picks one of: fold or call. (choice is announced to all players)
  - If Alice chooses 'call' (public): Alice matches the bet. If they cannot match the full amount, they go all-in and only the matched portion from each player remains in the pot.
  - Otherwise, if Alice chooses 'fold':
    The entire pot is given to Bob.
    Then, the game ends: Bob wins after Alice folds.

### Post-Betting Phase
- Post-betting events may fire based on game state. Each of the following conditions is evaluated top-to-bottom at its own step; every condition whose check passes at that moment performs its associated action. The conditions are not mutually exclusive: more than one may fire in the same phase.
  - If the current pot is more than 2 chips (public): Perform **Simultaneous Round (post-betting)** steps (both players participate per this sub-phase's own rules), then continue.
  - If Alice's hand contains a King (the deck's top rank) (public): Perform **Auction Round: Card Draw (post-betting)** steps (both players participate per this sub-phase's own rules), then continue.

#### Sub-phase: Simultaneous Round (post-betting) *(called from Post-Betting Phase)*
- All players choose simultaneously and in secret. No player knows the others' choices until all are locked in. Once all choices are submitted, each player's choice is publicly revealed, then the combined outcome is resolved and announced publicly. If a player fails to choose, a uniformly random option is selected for them.
- Alice chooses one of the following options: Press or Retreat.
- Bob chooses one of the following options: Press or Retreat.
- Outcomes based on choices:
  - If Alice chooses 'Press' AND Bob chooses 'Retreat': Bob peeks at 1 card in Alice's hand (selected uniformly at random). The card remains in Alice's hand. The peek itself is announced to all players (occurrence is public); only Bob sees which card was observed (content is private). If Alice's hand is empty, Bob is informed that it is empty.
  - If Alice chooses 'Retreat' AND Bob chooses 'Press':
    - If Alice's highest-ranked card has a higher rank than Bob's highest-ranked card: Bob pays 2 chips to Alice. If Bob has fewer than 2 chips, only the available amount is transferred.
    - Otherwise: Alice pays 1 chip to Bob. If Alice has fewer than 1 chip, only the available amount is transferred.
    *(The branch condition is evaluated privately; which branch fires is not announced directly.)*
  *(Note: different branches produce different observable chip effects; the branch taken may be partially inferable from chip changes.)*
  - For all other combinations (Press/Press, Retreat/Retreat): Bob draws 1 card from the Deck. Bob sees the card identity; the Deck-size decrement is public, signaling to both players that a draw occurred.
*(Play returns to **Post-Betting Phase**.)*

#### Sub-phase: Auction Round: Card Draw (post-betting) *(called from Post-Betting Phase)*
- Sealed-bid auction. Each player secretly picks a bid from 0 to 3 chips; a bid larger than the player's current chip stack is first clamped down to the stack size, so their effective bid (and the amount they pay if they win) never exceeds what they hold (all-in). Both bids are then revealed at the same moment. If both effective bids are 0, no one wins and no chips move. Otherwise the higher effective bid wins, with ties between nonzero bids broken by a coin flip; the winner pays their effective bid into the pot and draws 1 card from the deck. If the deck is empty at the moment the prize is to be performed, the auction is cancelled: the winner does not pay their bid and no chips move. Auctions do not collect an ante.
- Alice chooses a bid amount (minimum 0 chips, up to 3 chips). The chosen amount is recorded as Alice's bid but is not transferred yet; a subsequent resolution step decides whether chips actually move (for example, a sealed-bid auction only charges the winner). If the submitted amount exceeds the legal maximum, the bid is clamped to the maximum (all-in or declared cap). If the submitted amount is malformed or below the minimum, the engine substitutes a uniform-random legal amount. In either case the submitting player is notified privately and play continues with the resolved amount.

```

```

- Bob chooses a bid amount (minimum 0 chips, up to 3 chips). The chosen amount is recorded as Bob's bid but is not transferred yet; a subsequent resolution step decides whether chips actually move (for example, a sealed-bid auction only charges the winner). If the submitted amount exceeds the legal maximum, the bid is clamped to the maximum (all-in or declared cap). If the submitted amount is malformed or below the minimum, the engine substitutes a uniform-random legal amount. In either case the submitting player is notified privately and play continues with the resolved amount.
*(Play returns to **Post-Betting Phase**.)*

### Showdown
- Both players' hands are revealed to all players. Showdown rules:
  - **Comparison:** compare cards by rank, highest first. The first rank that differs determines the winner.
  - **Ties:** if highest cards match, compare next-highest (and so on). If all compared ranks tie and both hands run out at the same time, the pot is split.
  - **Unequal hand sizes:** if one player runs out of cards to compare first, the player with the remaining card wins that step.
  - **Empty hand:** an empty hand loses to any non-empty hand; two empty hands tie.
  - (Rank values: J=11, Q=12, K=13.)
- The showdown winner takes the entire pot. On a tie, each player receives half the pot (rounded down); any remaining odd chip is awarded uniformly at random to one tied player.
- The game ends: Showdown complete.

```

Per-turn observation prompt. Each time it is an agent’s turn, the engine sends the model a single user message that contains three pieces of information. The first describes the current state of the game: which phase we are in, the agent’s own hand, any public cards on the board, every player’s chip stack, the current pot, role or position assignments, and who the opponents are. The second is a chronological log of everything that has happened in the hand from the agent’s point of view: every public event plus every private observation the agent was entitled to see. The third describes the decision the agent has to make: the move type, the menu of legal actions allowed by the current phase, and the format the response should take. The agent is asked to reply with a single line of JSON of the form `{"action": <chosen_option>}`. Handling of malformed responses and the resulting fallback rate are described in more detail in Appendix F.

C Complexity axes (formal)

Each axis is a single scalar computed from a fixed precise-tier measurement budget per game. We run three thousand random-play episodes, denoted L0, and one thousand five hundred episodes of an L1 best-response policy to L0, used for the policy-perturbation axes. The opponent-modeling axis uses three hundred twenty opponent policies drawn from a low-discrepancy Sobol sequence on the strategy simplex, which we refer to as the *Sobol budget*.⁶ For each axis below we give the closed-form score plus one sentence on what it measures and how to read it, with symbols defined where they appear.

We use a single notational convention throughout. An information state $I_p = (dt, \text{hand}, \text{action path}, \text{chip bin}, \text{signals}, \text{roles})$ encodes a player’s full visible context, with decision type $dt = (\text{phase}, \text{move type}, \text{move name})$ as its first component, so $dt(I_p)$ recovers the decision type. Where an axis aggregates at the coarser dt level (because its inner quantity is defined per decision type), we sum over dt . Where an axis is naturally defined per information state (because the inner quantity, e.g. EV-vs-floor, is meaningful only at the situation level), we sum over visited I_p .

State space (\log_{10}). A measure of how many distinct observable contexts a player can reach. We approximate it by a Monte-Carlo draw rather than by exhaustive enumeration. Across the three thousand random-play episodes that make up the L0 budget, we record every information state I_p that each player actually visits and count the number of distinct ones.

$$\text{state_space}_{\log_{10}} = \log_{10} \left(\sum_p |\mathcal{I}_p| \right),$$

where \mathcal{I}_p is the set of distinct information states visited by player p across the L0 episode log. The count is a lower bound on the true reachable state space, since states the random-play distribution does not reach within three thousand episodes are undercounted. In practice the random-play distribution

⁶A Sobol sequence is a low-discrepancy alternative to uniform random sampling that gives more even coverage of the simplex at a smaller sample size. The 2,000-game candidate pool is scored at a faster tier (one thousand L0 episodes per game and sixty-four Sobol opponent policies instead of the precise tier’s three hundred twenty) so that farthest-point sampling can run at scale, and the 50 benchmark games are then re-scored at the precise tier. The precise values are the ones used throughout. Pool selection is unaffected because benchmark seeds were already chosen under fast-tier coordinates and the precise-tier re-score only refines them.

covers the contexts that an LLM is likely to face in play. Larger values correspond to more distinct contexts visited. The base-ten logarithm compresses a hundred-fold range in the raw count into one unit on the reported axis.

Temporal depth. Whether decisions early in an episode have downstream consequences, i.e. whether the player must plan forward rather than play myopically. Indexing decision types by $d = (\text{phase}, \text{move type}, \text{move name})$, we measure three per-type quantities on the L0 episode log:

- $f_d = n_d/n_{\text{eps}}$, the average number of times decision type d fires per episode, where n_d counts visits and n_{eps} is the episode count.
- η_d^2 , the share of final-payoff variance attributable to which action is chosen at d . Writing U_e for the focal player’s final payoff on episode e , $\bar{U}_{a,d}$ for the mean payoff over episodes that took action a at d , and \bar{U}_d for the overall mean at d , the standard one-way-ANOVA explained-variance ratio is

$$\eta_d^2 = \frac{\sum_a n_{a,d} (\bar{U}_{a,d} - \bar{U}_d)^2}{\sum_e (U_e - \bar{U}_d)^2}.$$

- r_d , the mean number of decisions the same player faces after d within the same episode.

The game-level temporal-depth score sums the product across decision types,

$$\text{temporal_depth} = \sum_d f_d \eta_d^2 r_d,$$

so a decision type contributes more when it fires often, has a strong action-choice signal, and leaves many subsequent decisions to follow. The reported axis is the raw score, not z -scored. It is non-negative and grows with both signal strength and lookahead horizon. Across the 50 benchmark games the raw score ranges from below 0.01, on myopic games such as canonical Kuhn poker, to approximately 0.76 on the deepest multi-round games in the collection, with a median of about 0.11.

Information sensitivity. How often the player’s optimal action depends on their private information.

$$\text{info_sens} = \sum_{I_p} \frac{f_{I_p}}{\sum_{I'_p} f_{I'_p}} \mathbf{1} \left[\arg \max_a \mathbb{E}[U \mid I_p, a] \neq \arg \max_a \mathbb{E}[U \mid dt(I_p), a] \right],$$

where the sum is over visited information states I_p and f_{I_p} is the number of L0 episodes in which I_p was reached (so visited states are weighted in proportion to how often they actually arise in play). The indicator inside the sum compares the argmax action when conditioning on the full information state I_p to the argmax action when conditioning only on the decision type $dt(I_p)$. A high score therefore means the player must condition their action on private information, while a low score means the same best action works across most information states at the same decision type. The score is bounded between zero and one.

Opponent modeling. How often the player’s optimal action depends on which opponent they face, i.e., whether best-response choice is stable across opponent policies or flips.

$$\text{opp_mod} = \sum_{dt} w_{dt} \left(1 - \text{modal_share}_\pi \left[\arg \max_a \mathbb{E}[U \mid dt, a, \pi] \right] \right),$$

where $w_{dt} = n(dt) / \sum_{dt'} n(dt')$ is the visit fraction of decision type dt and π ranges over three hundred twenty opponent policies drawn from a Sobol sequence on the strategy simplex. Of these, sixty-four are drawn from a single Sobol pass that gives even global coverage of the simplex. The remaining two hundred fifty-six are drawn from a second Sobol pass concentrated on regions of the simplex where the modal best response from the first sixty-four policies was unstable, so that more opponent diversity is used to test best-response stability where it appears most fragile. We run thirty-two playout episodes against each sampled opponent. The function `modal_share` is the share of opponents for whom the same action is the argmax. The score is bounded between zero and one. Zero means one action is the best response across every opponent, so the player has no need to model the opponent, and higher values mean the player must condition their strategy on opponent behavior.

Risk. The visit-weighted cost, expressed in payoff standard deviations, of switching from the expected-value-maximizing action to the action that maximizes the worst-decile payoff floor:

$$\text{risk} = \sum_{I_p} w_{I_p} \frac{\text{EV}(a_{I_p}^*) - \text{EV}(a_{\text{safe}, I_p})}{\sigma_U},$$

where the sum runs over visited information states I_p with at least twenty visits and at least two actions each tried at least five times, w_{I_p} is the visit fraction of I_p , and the score is then averaged across both player seats.⁷ Within an I_p , $a_{I_p}^* = \arg \max_a \text{EV}(a)$ is the expected-value-maximizing action and $a_{\text{safe}, I_p} = \arg \max_a q_{0.10}(a)$ is the action that maximizes the tenth-percentile payoff floor. The I_p contributes zero whenever $a^* = a_{\text{safe}}$, i.e., when no expected-value-versus-floor tradeoff is present. The denominator σ_U is the standard deviation of the realized utility U across L0 episodes. Values below 0.01 are reported as zero. The score is non-negative, with larger values indicating that the expected-value-maximizing action exposes the player to substantially worse worst-decile outcomes than the safest alternative. We aggregate at I_p rather than at dt because the EV-vs-floor tradeoff is only meaningful conditional on a specific hand and action path. Averaging EVs across heterogeneous information sets at the same dt would mix qualitatively different decisions into a single bucket.

Brittleness (\log_{10}). How much a small perturbation to the focal player’s L1 policy at a single decision type swings realized payoff.

$$\text{brittleness}_{\log_{10}} = \log_{10} \left(\sum_{dt} w_{dt} \frac{|\hat{\beta}_{dt}|}{\sigma_U} \right),$$

where $\hat{\beta}_{dt}$ is the OLS slope of the per-trial payoff change ΔU regressed on a perturbation indicator, equal to one if dt was the perturbed decision type and zero otherwise. We run twenty such trials per game. In each trial, three percent of the focal player’s L1 policy mass at one decision type is shifted to a uniform-random alternative action, and the opponent is held fixed at ten Dirichlet-random policies (uniform random points on the probability simplex) with fifteen playout episodes per opponent. The score is then averaged across the two focal seats. Larger values correspond to small policy perturbations producing larger payoff swings. Values near zero correspond to a payoff swing of one standard deviation per unit of policy-mass perturbation.

D Variance-inflation factors for the six axes

The variance inflation factor, or VIF (see Section 3.1), is a standard collinearity diagnostic. For each axis, we regress it on the other five (across the 50 benchmark games) and report $\text{VIF} = 1/(1 - R^2)$, where R^2 is the coefficient of determination of that regression. A VIF of one means the axis is linearly independent of the others, and a VIF of five is the conventional threshold above which collinearity is severe enough to inflate joint-regression standard errors. The per-axis values on the 50-game benchmark are as follows.

Axis	VIF (50-game benchmark)
State space (\log_{10})	3.31
Temporal depth	1.97
Information sensitivity	2.70
Opponent modeling	1.45
Risk	1.24
Brittleness (\log_{10})	1.19

All six VIFs are below the conventional collinearity threshold of five. The two largest are state space, at 3.31, and information sensitivity, at 2.70. This is consistent with the positive correlation between those two axes: richer state spaces tend to create more contexts in which private information shifts the best action. Risk and brittleness are near 1.2 and are nearly independent of the other axes.

⁷For visit-density reasons, the risk-axis aggregator coarsens I_p to its strategic-context subset (dt , hand, action path, chip bin), dropping signals and roles. The full I_p would fragment the per-bucket sample below the minimum-visit threshold on most games.

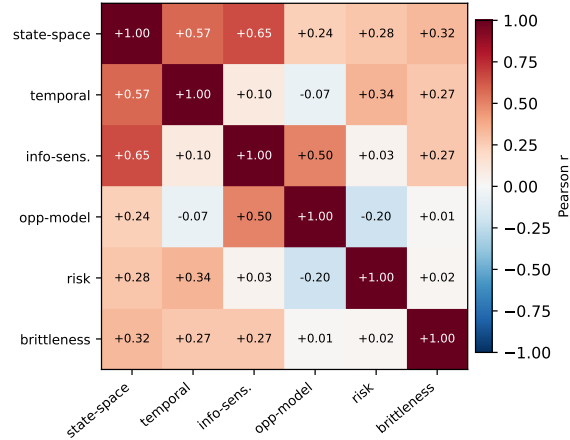


Figure 5: **Pairwise Pearson correlation of the six complexity axes across the 50 benchmark games.** The strongest positive pair is state space and information sensitivity, with Pearson $r = 0.65$, followed by state space and temporal depth at $r = 0.57$ and information sensitivity and opponent modeling at $r = 0.50$. Risk and brittleness are nearly independent of the remaining axes. In both cases the absolute correlation with every other axis is at most 0.34. All correlations stay below the conventional $|r| \approx 0.7$ threshold above which joint-regression standard errors begin to inflate substantially, and the per-axis VIFs reported in the table above are all below four.

E FPS coverage scatter

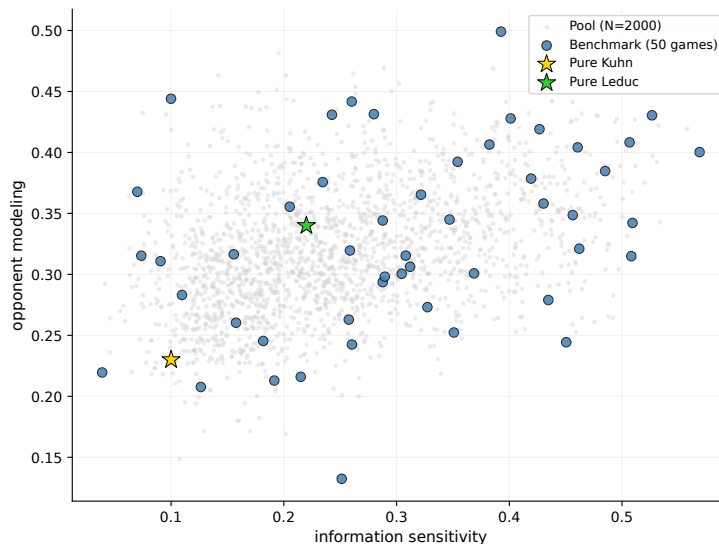


Figure 6: The 2,000-game accepted pool vs. the 50 FPS-selected benchmark games in two diagnostic axes (information sensitivity \times opponent modeling).

F Fallback-rate diagnostics

A *fallback* is a per-move event in which the engine could not recover a legal action from the model’s reply. Each model response is first passed through a strict JSON parser. If that fails, a lenient parser tries to recover the chosen action from common malformations (stray whitespace, trailing commentary, partial JSON). If both parsers fail, the engine substitutes a uniformly random legal action so play does not stall, and the move is recorded as a fallback. Each tournament slot records

per-seat counts of fallbacks and total moves. We aggregate to model-level rates over the merged 9-model tournament data.

Model	slots	moves	fallbacks	move rate	slot rate
gpt-5	3,679	8,508	43	0.51%	1.2%
gemini-3.1-flash-lite	9,516	23,022	84	0.36%	0.9%
gemini-2.5-pro	9,400	21,974	9	0.04%	0.1%
gemini-3.1-pro	9,475	22,156	9	0.04%	0.1%
deepseek-v3.1	9,424	22,786	8	0.04%	0.1%
claude-sonnet-4-6	3,757	8,524	0	0.00%	0.0%
gemma-4-31b	9,517	22,771	0	0.00%	0.0%
qwen-3.5	9,468	21,690	0	0.00%	0.0%
llama-3.3-70b	9,638	25,173	0	0.00%	0.0%

Move rate is the number of fallback-triggered moves divided by total moves. Slot rate is the fraction of slots with at least one fallback move.

The overall observation is that fallback rates are uniformly low: the worst offender (gpt-5) triggers the parser fallback on 0.5% of moves, and four of nine models record zero fallbacks across the set of 50 games. The leaderboard ordering is therefore not driven by parser-format compliance differences.

G Variance decomposition

Per-game strength estimates. We decompose variance across (model, game) pairs using per-game strength estimates $\hat{\alpha}_{m,g}$ from a per-game refit of the additive paired-comparison model, rather than the raw mean win margin of model m on game g . The refit subtracts off the opponent’s strength on g , so a model that happened to draw weaker opponents on game g is not credited with a higher per-game strength on that account. The raw mean would carry that opponent-mix bias straight into the decomposition. For each game g , we restrict the slot-level rows to matches played on g and refit

$$y_s = \alpha_{i^{(s)},g} - \alpha_{j^{(s)},g} + \varepsilon_s, \quad \sum_m \alpha_{m,g} = 0,$$

by OLS on the matches played on g . The resulting $\hat{\alpha}_{m,g}$ is model m ’s strength on game g adjusted for which opponents it faced on that game (the same adjustment the overall $\hat{\alpha}_m$ makes across the full tournament data). All $9 \times 50 = 450$ (model, game) pairs are identified on the full tournament data; in the 8-model (llama-excluded) subset 394 of 400 (model, game) pairs are identified, with the 6 unidentified pairs being (model, game) pairs whose only matches were against llama.

Decomposition. Let $\bar{\alpha}_{m\cdot}$ be the per-model average of $\hat{\alpha}_{m,g}$ across games, $\bar{\alpha}$ the grand mean, and $\bar{\alpha}_{\cdot g}$ the per-game average across models (which is identically zero by the sum-to-zero contrast, so the game main effect $\sigma_G^2 = \frac{1}{|G|} \sum_g (\bar{\alpha}_{\cdot g} - \bar{\alpha})^2$ is zero by construction and we omit it). The two non-trivial components are⁸

$$\sigma_M^2 = \frac{1}{|M|} \sum_m (\bar{\alpha}_{m\cdot} - \bar{\alpha})^2, \quad \sigma_{MG}^2 = \frac{1}{|M||G|} \sum_{m,g} (\hat{\alpha}_{m,g} - \bar{\alpha}_{m\cdot} - \bar{\alpha}_{\cdot g} + \bar{\alpha})^2.$$

All $9 \times 50 = 450$ (model, game) pairs are identified on the full tournament data, so the decomposition is computed on the balanced grid. In the 8-model llama-excluded subset, 394 of 400 pairs are identified (the six unidentified pairs are (model, game) pairs whose only matches on that game were against llama).

We compute 95% confidence intervals from a within-cell bootstrap of two thousand replicates. A cell is a (model, game) pair; for each cell we resample its contributing slot edges with replacement to the original cell size, refit the per-(model, game) cell mean, and re-decompose the resulting variance components. This differs from the paired-cluster bootstrap on (game seed, run id) clusters that we use elsewhere in the paper for $\hat{\alpha}$ and the capability-profile slopes, and we use the within-cell design

⁸The technique is standard two-way variance decomposition into row main effect, column main effect, and row \times column interaction. The per-model row average around the grand mean gives σ_M^2 , and the residual cell variation after subtracting both row and column averages gives σ_{MG}^2 .

here specifically because the paired-cluster bootstrap is biased upward for variance-components targets: replicates in which some cells end up with fewer-than-original slot counts inflate apparent model×game interaction variance. The within-cell design preserves cell coverage exactly on each replicate. We report the bias-corrected percentile interval.

Quantity	Full 9 models		Llama-excluded	
	point	95% CI	point	95% CI
σ_M^2	0.86	[0.76, 0.96]	0.19	[0.14, 0.25]
σ_{MG}^2	0.42	[0.31, 0.55]	0.25	[0.15, 0.37]
σ_{MG}^2/σ_M^2	0.49	[0.36, 0.65]	1.29	[0.64, 2.19]

The interaction-vs-model-main-effect ratio is 0.49 on the full 9-model tournament data and 1.29 when llama is excluded. With llama the leaderboard signal clearly dominates (CI well below 1); without llama, interaction is roughly comparable to the model main effect (CI straddles 1), so we cannot determine which is larger at the available power. See Section 6 (*Variance decomposition*) for discussion in main text.

H Robustness checks

Leave-one-game-out. We refit $\hat{\alpha}$ dropping each game in turn. Kendall τ between the leave-one-out (LOO) ranking and the full-data ranking has mean 0.998, minimum 0.944, with 48/50 LOO refits preserving the overall ranking exactly.

$\hat{\alpha}$ vs. coverage. To check whether models with more slots receive systematically higher or lower $\hat{\alpha}$, we plot per-model $\hat{\alpha}$ against the number of slots n_{slots} contributed by that model. We find no monotone relationship, so coverage imbalance does not predict rank.

Llama-excluded refit. llama-3.3-70b-together has outlier performance, so we exclude it (the bottom outlier) and refit on the remaining 8 models. The order of the 8 surviving models is preserved.

Table 3: **Llama-excluded leaderboard.**

Llama-excluded refit — $\hat{\alpha}$ (chips/game)		
Model	$\hat{\alpha}$ (no llama)	95% CI
gpt-5-4-high	+0.56	[+0.45, +0.67]
gemini-3.1-pro-preview	+0.49	[+0.42, +0.56]
claude-sonnet-4-6-max	+0.30	[+0.19, +0.41]
gemini-2.5-pro	+0.07	[+0.00, +0.15]
gemma-4-31b-it	−0.03	[−0.11, +0.04]
deepseek-v3.1	−0.22	[−0.29, −0.14]
gemini-3.1-flash-lite	−0.52	[−0.60, −0.43]
qwen-3.5	−0.65	[−0.74, −0.57]

Paired-cluster bootstrap 95% CI ($B=2,000$), sum-to-zero contrast. Refit on the 8 non-llama models.

The relative ranking of the 8 surviving models is identical to their relative position in the overall (with-llama) leaderboard (Table 1); the level shifts because the sum-to-zero contrast is now centered on a different population (no llama at -2.37 to anchor the bottom), so several mid-pack models flip sign relative to the new mean. The qualitative claim that gpt-5 and gemini-3.1-pro are at the top, and qwen-3.5 and gemini-3.1-flash-lite are at the bottom, holds in both specifications.

Bradley-Terry on win indicator. A logistic win-probability model on the indicator $1[\text{edge} > 0]$ yields per-model Bradley-Terry (BT) scores. Unlike the win-margin $\hat{\alpha}$, BT measures frequency

of winning rather than magnitude of margin, so the two estimators answer different questions. On our tournament data the BT ranking diverges noticeably from the win-margin ranking: several mid-pack models that win frequently with small margins (`gemin-2.5-pro`, `gemin-3.1-flash-lite`) score high on BT, while models that win less often but with large margins (`gpt-5`, `gemin-3.1-pro`) score lower on BT than on win-margin $\hat{\alpha}$. We report win-margin $\hat{\alpha}$ as the overall estimator because (i) we explicitly instructed models to maximize expected chips and (ii) win margin contains more information about model play during the game than the binary win indicator. The divergence from BT is itself a finding. The way a model considers the tradeoff between winning frequently with small margins and winning less often with large margins is worth reporting for follow-up work.

I Per-tertile leaderboards (composite-complexity split)

The composite-complexity axis is the first principal component of the 9×6 matrix of per-model axis-slopes $\hat{\beta}_{m,a}$ from the capability-profile regression in Section 7, a multivariate OLS of per-game strength $\hat{\alpha}_{m,g}$ on the six z -scored axes. The per-axis weights are +0.72 for brittleness-log10, +0.45 for state-space-log10, +0.41 for information-sensitivity, +0.29 for opponent-modeling, +0.15 for temporal-depth, and +0.09 for risk. Per-game composite scores sort the 50-game benchmark into three tertiles of 16, 17, and 17 games. Within each tertile we refit $\hat{\alpha}$ on the slot rows restricted to that tertile’s games, with paired-cluster bootstrap 95% CIs ($B=500$).

Table 4: Per-tertile additive paired-comparison leaderboards.

Per-tertile leaderboards — $\hat{\alpha}$ by composite-complexity tertile			
Model	$\hat{\alpha}_{T1}$	$\hat{\alpha}_{T2}$	$\hat{\alpha}_{T3}$
<code>gpt-5-4-high</code>	+0.35	+1.01	+1.19
<code>gemin-3.1-pro-preview</code>	+0.35	+0.93	+1.18
<code>claude-sonnet-4-6-max</code>	+0.24	+0.60	+1.02
<code>gemin-2.5-pro</code>	+0.26	+0.27	+0.57
<code>gemma-4-31b-it</code>	+0.21	+0.33	+0.19
<code>deepseek-v3.1</code>	+0.04	+0.06	+0.14
<code>gemin-3.1-flash-lite-preview</code>	+0.01	-0.41	-0.45
<code>qwen-3.5</code>	+0.05	-0.60	-0.51
<code>llama-3.3-70b-together</code>	-1.52	-2.18	-3.32

T1 = easiest 16 games, T2 = middle 17, T3 = hardest 17, by composite complexity. Paired-cluster bootstrap 95% CI widths ($B=500$) reach at most 0.53 chips/game across all 27 cells (widest on `claude-sonnet-4-6-max`, T3), with a median width of 0.28. The leaderboard is broadly stable across tertiles, but the top-3 and bottom-3 are not preserved exactly. On T1, `claude` drops out of the top-3 (`gpt-5`, `gemin-3.1-pro`, and `gemin-2.5-pro` are the top three at +0.35, +0.35, and +0.26 respectively) and `deepseek` replaces `qwen` in the bottom-3. On T2 and T3 the top-3 ordering settles into `gpt-5`, `gemin-3.1-pro`, `claude`, and win-margin gaps widen with complexity.

J Pairwise head-to-head table (full 9×9)

Table 5: Pairwise mean win margin: row – column, across the 50 benchmark games with both seats balanced. Bold = 95% paired-cluster bootstrap CI excludes 0 ($B=500$). Rows and columns sorted by leaderboard rank.

	gpt-5	gemini-3.1-pro	claude-sonnet-4-6	gemini-2.5-pro	gemma-4-31b	deepseek-v3.1	gemini-3.1-flash-lite	qwen-3.5	llama-3.3-70b
gpt-5	–	+0.22	+0.45	+0.28	+0.54	+1.01	+0.92	+1.00	+3.22
gemini-3.1-pro	–0.22	–	+0.17	+0.42	+0.58	+0.73	+0.83	+1.31	+3.54
claude-sonnet-4-6	–0.45	–0.17	–	–0.01	+0.40	+0.68	+1.20	+0.77	+3.26
gemini-2.5-pro	–0.28	–0.42	+0.01	–	+0.07	+0.17	+0.76	+0.60	+2.71
gemma-4-31b	–0.54	–0.58	–0.40	–0.07	–	+0.14	+0.45	+0.74	+2.54
deepseek-v3.1	–1.01	–0.73	–0.68	–0.17	–0.14	–	+0.46	+0.22	+2.32
gemini-3.1-flash-lite	–0.92	–0.83	–1.20	–0.76	–0.45	–0.46	–	+0.33	+1.79
qwen-3.5	–1.00	–1.31	–0.77	–0.60	–0.74	–0.22	–0.33	–	+2.08
llama-3.3-70b	–3.22	–3.54	–3.26	–2.71	–2.54	–2.32	–1.79	–2.08	–

Fifty-eight of the 72 off-diagonal entries reach significance at the 95% level (paired-cluster bootstrap, $B=500$).

K Solver-baseline reference matchups (full)

For five benchmark seeds, we obtained reasonable tabular CFR⁺ abstractions and solved to convergence within them. The resulting abstracted-solver policies are not Nash policies of the original games (finite abstraction introduces residual exploitable error), so we treat them only as a third-perspective sanity check alongside the LLM-vs-LLM tournament. We play each of the 9 LLMs against the abstracted CFR⁺ solver on each of the 5 seeds, targeting $n_{\text{slots}}=100$ paired slots per (model, seed) matchup; the merged dataset is 4,494 slots (45 (model, seed) matchups × 100 nominal, minus 6 claude-sonnet-4-6-max slots that failed at the provider and were not retried: 5 missing on seed 933 and 1 on seed 10137). Top-ranked models post small positive average margins (+0.30 to +0.58 chips/game), consistent with finding and exploiting residual abstraction error; llama-3.3-70b is the only model that the solver consistently exploits, with an average of –1.89 chips per game across the five seeds and a low of –3.18 chips per game on the most complex seed. The per-model averages rank-correlate strongly with the overall LLM-vs-LLM leaderboard, with Spearman $\rho = 0.95$ and $p = 0.0001$.

We report each model’s edge against the abstracted solver as $\bar{y} \pm \text{SE}$, the mean chip margin per paired-play-seed group with paired-seat standard error. The game is zero-sum, so the model edge \bar{y} already pins down the solver’s loss as $-\bar{y}$. The CFR⁺ solver policy is the average strategy of CFR⁺ run to convergence within the abstraction (default lumping for four seeds, finer abstraction for seed 11520). Decisions are sampled stochastically from the mixed strategy. We target one hundred paired slots per (seed, model) matchup. The achieved count is one hundred in 43 of 45 matchups, with 95 in the (seed 933, claude-sonnet-4-6-max) matchup and 99 in the (seed 10137, claude-sonnet-4-6-max) matchup, in both cases due to provider-side failures that were not retried.

Table 6: **LLM-vs-abstracted-CFR⁺ reference matchups, 5 seeds with tractable solver abstractions × 9 models, 50 paired-play-seed runs (≤ 100 slots) per (model, seed) matchup.** Each cell is the mean chip margin of the model against the solver on that seed, averaged over the paired-play-seed groups (the two seat assignments within a group are collapsed by within-group mean), ± the paired-play-seed standard error (standard deviation of the group means divided by $\sqrt{n_{\text{groups}}}$, where n_{groups} is the number of distinct play-seed groups for that (model, seed) cell). The final column is the per-model average across the 5 seeds. The CFR⁺ policy is the solver output on a finite abstraction, so any residual exploitable error in the abstracted policy can be picked up by the model and shows up here as a positive edge.

Model	seed 5149 <i>simple</i>	seed 11520 <i>simple</i>	seed 933 <i>low-med</i>	seed 10137 <i>medium</i>	seed 12140 <i>upper-med</i>	avg
gpt-5	+0.40 ±0.09	+0.36 ±0.07	+1.20 ±0.65	+0.64 ±0.18	+0.30 ±0.23	+0.58
claude-sonnet-4-6	+0.30 ±0.07	+0.38 ±0.07	+0.46 ±0.76	+0.46 ±0.20	+0.42 ±0.52	+0.40
gemini-2.5-pro	+0.16 ±0.10	+0.52 ±0.11	+1.00 ±1.03	+0.40 ±0.22	-0.50 ±0.25	+0.32
gemini-3.1-pro	+0.18 ±0.13	+0.42 ±0.08	-0.24 ±0.97	+0.62 ±0.20	+0.54 ±0.42	+0.30
gemma-4-31b	+0.24 ±0.08	+0.42 ±0.08	+0.08 ±0.78	+0.06 ±0.25	-0.56 ±0.43	+0.05
deepseek-v3.1	+0.22 ±0.10	+0.38 ±0.10	-0.12 ±0.52	+0.02 ±0.24	-0.34 ±0.15	+0.03
gemini-3.1-flash-lite	+0.22 ±0.17	+0.48 ±0.09	+0.26 ±0.87	+0.26 ±0.27	-1.32 ±0.37	-0.02
qwen-3.5	+0.10 ±0.13	+0.36 ±0.07	+0.10 ±0.86	-0.82 ±0.32	-0.82 ±0.50	-0.22
llama-3.3-70b	-1.04 ±0.25	-0.36 ±0.15	-2.20 ±0.96	-2.66 ±0.41	-3.18 ±0.74	-1.89

Per-model averages across the 5 seeds rank-correlate strongly with the LLM-vs-LLM overall leaderboard (Spearman $\rho=0.95$, $p=0.0001$; Pearson $r=0.98$, $p<0.0001$), indicating the solver baseline and the peer tournament are measuring essentially the same underlying axis of strategic competence on this distribution.

L Full per-axis regression table

Table 7 reports the same per-model multivariate OLS slopes plotted in Figure 3, in tabular form. CIs are paired-cluster bootstrap ($B = 500$); p -values are Benjamini–Hochberg corrected at FDR 0.05 across the full family of $9 \times 6 = 54$ (model, axis) coefficients. Bold entries clear BH.

Table 7: Per-model multivariate OLS slope of $\hat{\alpha}_{m,g}$ on each z -scored axis, controlling for the other five axes. Bold = BH-adjusted $q < 0.05$ across the 54 coefficients.

	state-sp.	temporal	info-sens.	opp-mod.	risk	brittle.
gpt-5	+0.13	+0.06	+0.10	+0.11	+0.03	+0.23
gemini-3.1-pro	+0.22	-0.05	+0.00	+0.13	+0.06	+0.15
claude-sonnet-4-6	+0.18	-0.05	+0.03	+0.13	+0.02	+0.27
gemini-2.5-pro	-0.12	+0.13	+0.13	+0.03	+0.08	+0.05
gemma-4-31b	+0.05	+0.05	+0.01	-0.04	-0.03	-0.06
deepseek-v3.1	-0.02	+0.03	+0.04	-0.02	+0.02	-0.01
gemini-3.1-flash-lite	-0.30	+0.18	+0.19	-0.14	-0.00	-0.15
qwen-3.5	+0.06	-0.16	-0.11	-0.15	-0.19	-0.05
llama-3.3-70b	-0.19	-0.19	-0.40	-0.05	+0.01	-0.42

M Capability profile in absolute units

The main-text radar (Figure 3) plots the per-(model, axis) slope $\hat{\beta}_{m,a}$ in chips/game per σ of axis, which is the local sensitivity of model m 's edge to axis a . The companion plot below uses the same fitted regression, but evaluates each model's predicted per-game strength on a synthetic game where axis a is at its observed maximum z -score and the other five axes are at their observed medians:

$$\hat{\alpha}_{m,g_a^*} = \hat{\beta}_{m,0} + \hat{\beta}_{m,a} z_a^{\max} + \sum_{a' \neq a} \hat{\beta}_{m,a'} z_{a'}^{\text{med}}.$$

Each spoke is then in chips/game on a benchmark-extreme game for that axis, rather than a per- σ slope.

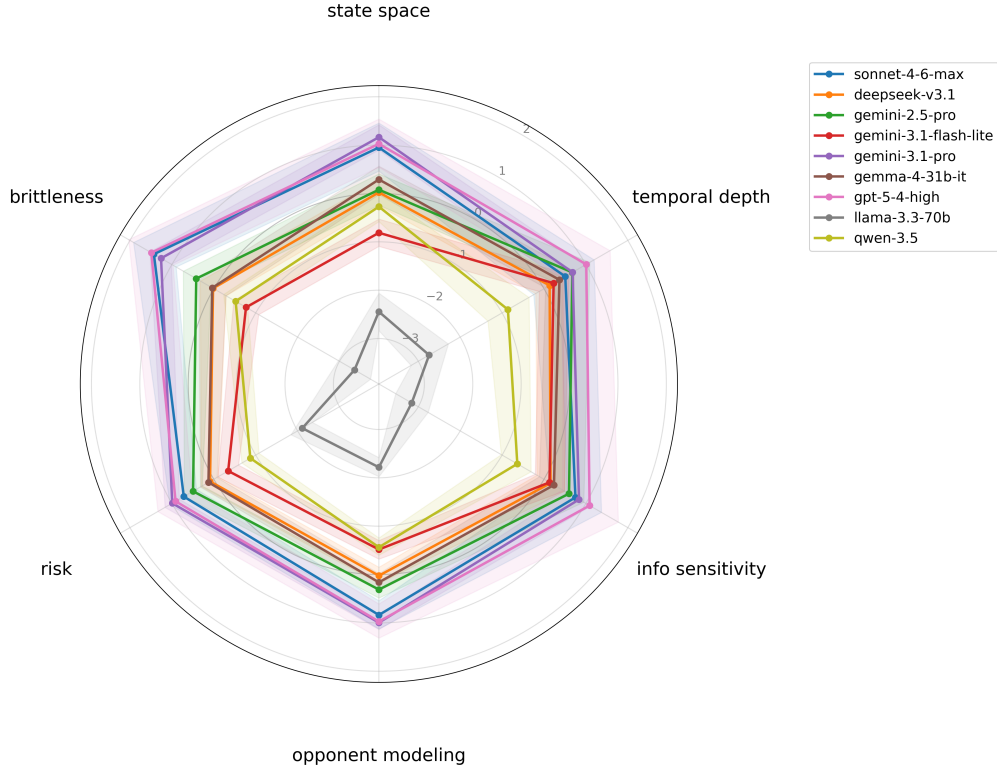


Figure 7: **Capability profile in absolute units.** Predicted per-game strength $\hat{\alpha}_{m,g_a^*}$ from the same multivariate OLS used for Figure 3, evaluated at the synthetic input defined above (each axis at its 50-game maximum z -score in turn, with the other five axes held at their 50-game medians). Units are chips/game versus the across-model mean. Shaded bands are 95% paired-cluster bootstrap CIs ($B=500$) propagated through the linear predictor.

Two contrasts come out of the absolute-units plot that the slope-only radar cannot show. First, the three top-leaderboard models are clearly above the across-model mean on the most-brittleness-heavy benchmark game (gpt-5-4-high at +1.49 chips/game, claude-sonnet-4-6-max at +1.43, gemini-3.1-pro-preview at +1.26), with gpt-5-4-high the flattest of the three across spokes (+0.91 to +1.49) and claude-sonnet-4-6-max the most peaked. Second, gemini-3.1-flash-lite-preview is the only direction-splitting profile: predicted above the mean on temporal-depth (+0.23) and information-sensitivity (+0.13) but below it on the other four axes, so on the most-temporal-depth game in the benchmark flash-lite is a real (small) winner rather than just a gap-narrower. The main-text radar suppresses both contrasts because it plots only the slopes.

N Local jaggedness: estimation, inference, and subset robustness

This section gives the full construction of the stakes-normalized local-jaggedness measure J_m used in Section 8, reports its sensitivity to the neighborhood size K , and reports the tournament-subset robustness check that motivates the choice of σ_g -only studentization.

Construction. The full formula for J_m is given in Section 8. The kNN aggregator uses the population (biased) standard deviation of the four neighborhood values, i.e. divides by $|\mathcal{N}(g)|$ rather than $|\mathcal{N}(g)| - 1$. Switching the convention to the sample standard deviation would multiply every J_m by $\sqrt{|\mathcal{N}(g)|/(|\mathcal{N}(g)| - 1)} \approx 1.155$ uniformly, so the choice of convention cancels out of any ranking, ratio, or bootstrap CI; we use the population convention for notational simplicity. We compute 95% confidence intervals from a bias-corrected paired-cluster bootstrap of 500 replicates, where clusters are indexed by (game seed, run id). At each replicate we resample clusters with

replacement, re-fit the global additive paired-comparison $\hat{\alpha}_m$ and the per-game refit $\hat{\alpha}_{m,g}$, recompute σ_g on the resampled rows, and recompute J_m . We report the bias-corrected percentile interval.

Sensitivity to the neighborhood size K . The main-text construction uses $K = 3$. We re-run the σ_g -only J_m pipeline at $K \in \{2, 4, 5, 7, 10, 15\}$. The nine-model mean of J_m rises smoothly with K as larger neighborhoods incorporate more cross-game variance, from 0.067 at $K = 2$ to 0.099 at $K = 15$, but the per-model ranking is extraordinarily stable. The Spearman rank correlation against the $K = 3$ ordering is +1.000 at $K = 2$ and at $K = 4$, and +0.983 at every larger K in the sweep. A single position swap, in which `claude-sonnet-4-6-max` and `qwen-3.5-together` swap ranks three and four, accounts for the entire departure from perfect agreement. `llama-3.3-70b-together` is the most locally volatile model at every K in the sweep, and `deepseek-v3.1` remains the smoothest.

Tournament-subset robustness. A concern is that a local-jaggedness measure of the form $J_m = \text{mean}_{g'} \text{std}\{z_{m,g'}\}$ depends on which models share the tournament pool, because both $\hat{\alpha}_{m,g}$ (the per-game refit) and $\hat{\alpha}_m$ (the global strength) are estimated on the shared pool. We test this directly by rerunning the σ_g -only J_m pipeline under four subset conditions: (i) leave-one-model-out, dropping each of the nine models in turn and recomputing J_m on the remaining eight; (ii) drop top three (`gpt-5`, `gemini-3.1-pro`, `claude`); (iii) drop bottom three (`llama-3.3-70b`, `qwen-3.5`, `gemini-3.1-flash-lite`); and (iv) mid-pack only (`gemini-2.5-pro`, `gemma-4-31b-it`, `deepseek-v3.1`).

Model	baseline	LOO mean	LOO min	LOO max	drop top3	drop bot3	mid3 only
<code>gpt-5</code>	0.092	0.095	0.091	0.101	–	0.068	–
<code>gemini-3.1-pro</code>	0.062	0.066	0.058	0.075	–	0.062	–
<code>claude-sonnet-4-6</code>	0.086	0.087	0.080	0.097	–	0.063	–
<code>gemini-2.5-pro</code>	0.047	0.049	0.048	0.053	0.061	0.066	0.057
<code>gemma-4-31b</code>	0.052	0.054	0.052	0.059	0.063	0.066	0.048
<code>deepseek-v3.1</code>	0.037	0.041	0.037	0.051	0.051	0.066	0.057
<code>gemini-3.1-flash-lite</code>	0.057	0.059	0.051	0.084	0.049	–	–
<code>qwen-3.5</code>	0.082	0.084	0.074	0.113	0.064	–	–
<code>llama-3.3-70b</code>	0.152	0.150	0.143	0.161	0.125	–	–

Under σ_g -only studentization, J_m is robust to which models share the tournament pool. For the high- J_m models the leave-one-out range across the eight subset replicates is tight, on the order of 10 to 20% of the baseline value (`gpt-5`, `claude-sonnet-4-6`, `llama-3.3-70b`). The low- J_m models have wider relative LOO ranges (up to roughly 40–60% of baseline for `deepseek-v3.1`, `qwen-3.5`, and `gemini-3.1-flash-lite`) because their small denominators amplify any absolute LOO shift; their absolute LOO shifts are themselves small. The qualitative ordering, with `llama-3.3-70b` most jagged, then `gpt-5`, `claude-sonnet-4-6`, and `qwen-3.5`, then the mid-pack and `deepseek-v3.1` smoothest, is preserved under every leave-one-out replicate. The drop-top-three, drop-bottom-three, and mid-three-only conditions move the absolute values somewhat more, but the inferential picture is unchanged.

O Per-game results

The full per-(model, game) pair-mean win margin across the 50-game benchmark, sorted ascending by composite complexity score. The `cmp1x` column is the simple mean of the six z -scored axis values for each game, so it is centered at zero across the 50-game benchmark by construction. Negative values denote games whose axis values are below the benchmark mean (Kuhn-like) and positive values denote above-mean games. This is a lightweight summary used only for sorting the rows of this table; the PC1-based composite used for the tertile leaderboards in Appendix I is a separate construction. All 9 models reach per-(model, game) coverage on all 50 seeds via the rotating-matchup schedule (Section 5).

Table 8: Per-(model, game) pair-mean win margin on the 50-game benchmark, sorted ascending by composite complexity. `cmplx` = mean of the six z -scored axes.

seed	cmplx	gpt-5	gemini-3.1-pro	claude-sonnet-4-6	gemini-2.5-pro	gemma-4-31b	deepseek-v3.1	gemini-3.1-flash-lite	qwen-3.5	llama-3.3-70b
10173	-3.01	+0.23	+0.73	-0.30	+0.47	+0.00	+0.07	-0.12	+0.56	-2.00
11517	-2.57	+0.00	+0.56	+0.88	+0.62	+0.00	+0.51	+0.00	+0.67	-2.66
2601	-2.38	+0.07	+0.73	-0.15	+0.62	+0.28	-0.19	+0.70	+0.39	-2.36
11784	-2.24	+0.55	+0.81	+0.68	+0.30	+0.32	+0.40	-0.20	-0.19	-1.93
963	-2.06	+0.00	+0.49	+0.00	+0.49	+0.09	+0.21	+0.07	+0.03	-1.64
11520	-2.02	+0.07	+0.16	-0.10	+0.00	+0.15	+0.20	+0.20	-0.01	-0.78
6586	-1.99	+0.30	+0.28	+0.80	+0.57	-0.07	+0.18	-0.06	+0.20	-1.40
4968	-1.98	+2.30	+1.07	+0.40	+0.88	+0.66	-0.42	-0.05	-0.31	-1.94
862	-1.95	+0.00	+0.61	+0.00	+0.47	+0.00	+0.28	+0.47	-0.01	-2.05
4426	-1.47	+0.15	+0.12	+0.05	+0.14	+0.04	+0.10	+0.00	-0.05	-0.33
2385	-1.44	+0.28	+0.39	+0.28	+0.25	-0.13	+0.04	+0.23	-0.11	-0.81
5470	-1.41	+0.30	+0.22	+0.10	+0.23	-0.06	+0.03	-0.11	-0.13	-0.50
5149	-1.33	-0.05	+0.16	+0.30	+0.12	+0.50	+0.31	-0.01	-0.29	-0.95
2522	-1.04	+0.00	+0.00	+3.00	+0.00	+0.59	+0.53	+0.69	+0.56	-2.60
10137	-0.91	+0.45	+1.79	+0.53	+0.22	+1.35	+0.66	+0.17	-0.50	-3.83
1608	-0.87	+1.25	+0.15	-0.15	+0.48	+0.48	+0.12	+0.19	+0.24	-1.99
7052	-0.81	-0.47	+1.37	+0.85	+0.70	+0.89	-0.19	-0.75	-0.17	-2.11
6903	-0.65	+0.22	+0.97	-0.35	+0.30	+0.36	-0.10	-0.14	-0.33	-1.20
2914	-0.64	+2.75	+2.31	-0.37	-0.34	-0.67	+0.44	-1.46	-1.25	+0.19
9548	-0.43	+0.57	+1.50	+0.40	+0.27	+0.28	+0.74	-0.33	-0.63	-2.17
7379	-0.39	+1.57	+1.42	+0.07	+0.96	+0.58	+0.87	-0.65	-0.12	-3.48
2345	-0.37	+0.80	+0.60	+0.45	+0.21	+0.35	-0.14	+0.12	-0.30	-1.19
9398	-0.04	+1.32	+1.59	+3.35	+0.81	+0.07	+0.55	-0.66	-1.23	-2.81
1949	+0.02	+1.60	+1.14	+0.00	+0.00	+0.61	+0.47	+0.82	-0.02	-3.39
2495	+0.13	+0.05	+0.17	+0.00	+0.38	-0.08	+0.06	-0.17	-0.42	+0.01
8297	+0.14	+0.00	+0.69	+0.62	-0.19	+1.54	+0.02	-0.24	-0.06	-2.31
1247	+0.15	+0.15	+1.38	+0.02	+0.35	+0.65	+0.03	-0.54	+0.44	-2.44
10738	+0.19	-0.05	+0.89	-0.10	+0.52	+0.16	-0.35	+0.20	-0.51	-1.04
2526	+0.20	+3.73	+2.84	+1.75	+1.59	+2.79	+0.06	-1.07	-2.16	-4.76
933	+0.31	+3.45	+1.44	+0.70	+0.74	-0.03	+0.55	-0.41	-0.61	-2.46
6635	+0.43	+2.23	+1.34	+1.77	+0.96	+0.15	+0.77	+0.01	-0.82	-3.05
10790	+0.57	+0.81	+0.55	+0.00	+0.84	+0.55	-0.31	-0.12	+0.03	-2.83
6520	+0.59	+0.38	+0.75	+1.25	+0.30	+1.06	+0.04	-0.53	-0.03	-2.50
8489	+0.83	+1.13	+0.98	-0.10	+0.78	+0.36	-0.67	+0.69	+0.24	-3.00
7142	+0.92	+0.72	+0.46	-0.05	+0.15	+0.54	-0.24	-0.14	+0.05	-1.00
12140	+0.94	+3.72	+2.02	+2.62	+0.99	-0.24	+0.55	-0.31	-0.78	-4.28
7830	+0.97	+0.40	+0.90	-0.60	+0.83	+0.79	+0.04	-0.11	-0.89	-2.36
203	+1.01	+5.00	+2.13	+0.61	+1.09	+1.89	+1.24	-0.80	-1.38	-4.68
3651	+1.17	+0.65	+1.98	+0.78	+0.89	-0.06	+0.60	+0.66	-0.66	-3.84
9754	+1.39	+0.10	+3.15	+2.32	+0.21	+1.27	-0.65	-1.04	-0.12	-3.95
3483	+1.48	+0.65	+1.43	+1.27	+0.55	+1.36	+0.32	-0.31	-1.10	-2.61
10427	+1.68	+0.77	+1.28	+3.42	+0.27	+0.95	-0.31	-0.16	+0.66	-4.05
5368	+1.69	+0.35	+0.45	+0.12	+0.38	+0.56	+1.06	+0.08	+0.04	-3.15
10786	+1.85	+0.60	+1.04	+0.05	+0.75	+0.13	+0.29	+0.12	-0.23	-2.71
1406	+1.97	+1.88	+1.69	+0.68	+1.83	+0.82	+0.59	-0.32	-0.51	-4.85
6644	+2.14	+1.35	+2.27	+1.80	+1.67	+0.20	+0.33	-0.65	-0.97	-3.58
4059	+2.19	+0.25	+0.72	+1.10	+0.69	+0.26	-0.01	+0.25	-0.17	-1.86
4643	+2.34	+3.38	+2.45	+1.45	+1.20	-0.10	-1.15	+1.38	-1.29	-3.22
10760	+2.87	+2.35	+2.03	+0.25	+2.47	-0.33	+0.66	-1.68	+0.25	-5.10
11435	+3.82	+0.28	+2.06	+6.05	+1.05	+0.45	+1.90	-0.49	+0.50	-6.24

P Per-cell $\hat{\alpha}_{m,g}$ matrix and rank-stability against a noise null

This appendix reports the full matrix of per-game strength estimates $\hat{\alpha}_{m,g}$ and tests whether the per-game variation in model rankings exceeds what sampling noise alone would produce. The per-cell point estimates are the same per-game additive paired-comparison refits used throughout the paper (Section 6). For each (model, game) pair we additionally compute a 95% bootstrap confidence interval from $B = 500$ paired-cluster bootstrap replicates on (game seed, run id) clusters.

Table 9 shows the point estimates only, sorted ascending by composite-complexity score. Models are column-ordered by the overall leaderboard.

Table 9: Per-game strength estimates $\hat{\alpha}_{m,g}$ (chips/game), per model. Rows are the 50 benchmark games sorted ascending by composite-complexity score, and columns are the models in overall leaderboard order.

seed	cmplx	gpt-5	gem-3.1-pro	claude-4-6	gem-2.5-pro	gemma-31b	deepseek	gem-flash	qwen-3.5	llama
963	-2.53	+0.33	+0.39	+0.08	+0.33	+0.21	+0.08	+0.26	-0.21	-1.49
5149	-2.25	+0.13	+0.27	+0.42	+0.18	+0.29	+0.03	-0.02	-0.33	-0.96
11520	-2.21	+0.17	+0.06	-0.03	+0.10	+0.12	+0.10	+0.09	+0.07	-0.68
6586	-2.08	+0.57	+0.27	+0.30	+0.32	-0.04	-0.05	+0.01	-0.13	-1.26
4426	-2.02	-0.16	+0.10	+0.07	+0.09	+0.10	+0.08	+0.01	+0.02	-0.31
11517	-1.86	+0.36	+0.16	+0.36	+0.22	+0.30	+0.27	+0.28	+0.44	-2.37
862	-1.75	+0.20	+0.29	+0.27	+0.31	+0.23	+0.00	+0.31	+0.20	-1.82
2385	-1.57	+0.08	+0.29	+0.10	+0.15	-0.02	-0.03	+0.17	-0.05	-0.68
10173	-1.45	+0.46	+0.48	+0.18	+0.35	+0.13	-0.11	+0.12	+0.15	-1.78
7379	-1.34	+1.27	+1.16	+0.49	+0.53	+0.12	+0.54	-0.45	-0.67	-2.99
2522	-1.24	+0.23	+0.24	+0.72	+0.22	+0.20	+0.14	+0.27	+0.26	-2.28
5470	-1.19	+0.20	+0.23	+0.17	+0.15	-0.08	+0.09	-0.13	-0.11	-0.54
11784	-1.13	+0.56	+0.34	+0.64	+0.30	+0.24	+0.08	-0.31	+0.01	-1.84
2601	-0.87	+0.29	+0.51	-0.00	+0.35	+0.15	+0.15	+0.33	+0.28	-2.04
4968	-0.80	+0.55	+0.68	-0.11	+0.58	+0.74	-0.54	-0.03	-0.12	-1.75
7142	-0.76	+0.21	+0.37	-0.21	+0.22	+0.47	-0.23	-0.16	+0.18	-0.87
2914	-0.59	+2.86	+1.53	+0.11	-0.54	-0.85	+0.04	-1.43	-1.14	-0.58
933	-0.57	+1.24	+0.94	+1.12	+0.37	-0.10	-0.07	-0.77	-0.53	-2.21
10137	-0.55	+1.32	+0.78	+0.76	-0.03	+0.87	+0.51	+0.28	-0.91	-3.59
1949	-0.48	+0.32	+0.69	+0.28	+0.33	+0.42	+0.15	+0.43	+0.37	-2.99
1247	-0.46	+0.62	+0.97	+0.47	+0.11	+0.56	-0.17	-0.23	-0.08	-2.23
1608	-0.39	+0.47	+0.31	+0.22	+0.29	+0.28	+0.27	-0.05	+0.01	-1.79
2345	-0.27	+0.48	+0.62	+0.44	+0.30	+0.17	-0.32	-0.05	-0.32	-1.32
7052	-0.18	+0.46	+1.26	+0.54	+0.61	+0.45	+0.10	-1.18	-0.31	-1.94
2495	-0.06	+0.10	+0.15	+0.02	+0.32	-0.06	+0.02	-0.08	-0.36	-0.11
2526	-0.00	+1.74	+1.48	+1.31	+0.78	+1.66	+0.18	-0.73	-2.25	-4.16
6903	+0.20	+0.23	+0.73	-0.12	+0.32	+0.31	-0.16	-0.16	-0.12	-1.02
12140	+0.20	+2.19	+1.45	+1.57	-0.22	-0.23	-0.18	-0.46	-0.56	-3.56
8297	+0.23	+0.84	+0.84	+0.57	-0.36	+1.03	+0.09	-0.20	-0.50	-2.32
10738	+0.31	-0.05	+0.71	+0.34	+0.44	+0.08	-0.06	-0.08	-0.47	-0.90
7830	+0.38	+0.81	+0.97	+0.21	+0.72	+0.56	+0.30	-0.24	-0.98	-2.35
3483	+0.47	+0.93	+0.60	+1.48	+0.49	+0.39	+0.28	-0.09	-1.51	-2.56
9548	+0.48	+0.54	+0.80	+0.80	+0.40	+0.09	+0.25	-0.47	-0.41	-2.01
9398	+0.66	+1.14	+1.26	+1.76	+0.67	-0.18	-0.02	-0.33	-1.45	-2.85
10786	+0.87	+0.78	+0.71	+0.76	+0.17	+0.37	-0.09	-0.14	-0.01	-2.55
203	+0.88	+0.80	+1.57	+1.94	+0.49	+1.09	+0.90	-0.66	-1.93	-4.20
8489	+0.89	+1.39	+0.53	+0.39	+0.71	-0.26	-0.21	-0.05	+0.27	-2.76
6635	+1.04	+0.89	+1.03	+0.96	+0.67	-0.32	+0.51	-0.03	-1.04	-2.66
6644	+1.05	+2.56	+1.23	+0.05	+1.21	+0.28	-0.20	-0.94	-0.89	-3.31
5368	+1.12	+1.00	+0.69	+0.97	+0.51	+0.32	+0.25	-0.35	-0.24	-3.16
10790	+1.14	+1.09	+0.78	+0.57	+0.47	+0.11	-0.06	-0.28	+0.05	-2.74
4059	+1.14	+0.44	+0.49	+0.39	+0.54	-0.01	+0.27	-0.17	-0.25	-1.69
6520	+1.27	+1.22	+0.57	+1.80	+0.21	+0.48	-0.11	-1.05	-0.35	-2.76
3651	+1.29	+1.24	+1.53	+0.59	+0.03	+0.20	+0.06	+0.24	-0.53	-3.35
4643	+1.50	+1.71	+1.52	+1.27	+0.38	-0.18	-0.45	+0.12	-1.50	-2.87
1406	+2.32	+1.64	+0.78	+0.94	+1.33	+0.18	+0.18	+0.08	-0.64	-4.48
9754	+2.42	+2.80	+1.97	+2.70	-0.68	+0.30	-0.12	-1.55	-1.24	-4.19
10427	+2.79	+0.80	+1.25	+1.82	-0.09	+0.12	+0.03	-0.74	+0.52	-3.72
11435	+2.91	+1.22	+1.56	+0.45	+0.33	+0.84	+1.24	+0.33	-0.38	-5.60
10760	+3.03	+2.65	+1.68	+2.22	+1.97	-0.63	-0.59	-1.08	-1.50	-4.71

Rank stability. The per-game rankings induced by $\hat{\alpha}_{m,g}$ are not identical to the overall leaderboard, and some pairs flip. We decompose this disagreement into a component attributable to sampling noise and a residual through three measurements.

The Kendall rank correlation between the per-game ranking and the overall ranking has a mean of 0.65 and a median of 0.72 across the 50 benchmark games. Three-quarters of games have a τ of at least 0.6, and a quarter have $\tau \geq 0.8$. The worst-case game has $\tau = 0.11$, the best $\tau = 0.89$. The overall ordering is therefore a strong but imperfect predictor of the per-game ordering.

The average number of pairwise rank reversals per game, against the overall leaderboard, is 6.22 out of $\binom{9}{2} = 36$ possible pairwise comparisons. The distribution is skewed, with median 5 reversals and maximum 16.

The noise-baseline comparison computes the expected number of those reversals under a null where the true per-game ranking equals the overall ranking and the only source of per-game disagreement is sampling noise on the per-cell $\hat{\alpha}_{m,g}$ estimates themselves. For each pair (m_i, m_j) on each game g , let $\widehat{\text{SE}}_{\text{pair}}(g)$ be the bootstrap-empirical standard deviation of $\hat{\alpha}_{m_i,g}^{(b)} - \hat{\alpha}_{m_j,g}^{(b)}$ across the 500 replicates. Under the null that the true difference equals the overall difference $\hat{\alpha}_{m_i} - \hat{\alpha}_{m_j}$, the probability of an observed reversal on that pair-game is

$$P_{\text{rev}}(i, j, g) = \Phi\left(-\frac{|\hat{\alpha}_{m_i} - \hat{\alpha}_{m_j}|}{\widehat{\text{SE}}_{\text{pair}}(g)}\right),$$

where Φ is the standard normal CDF. Let $E_g = \sum_{i < j} P_{\text{rev}}(i, j, g)$ denote the expected reversal count on game g under this null (the sum across all 36 unordered pairs), and let $V_g = \sum_{i < j} P_{\text{rev}}(i, j, g)(1 - P_{\text{rev}}(i, j, g))$ denote its variance.⁹

Averaged across the 50 benchmark games, the expected reversal count under the null is 3.71, compared to the observed 6.22. The observed-to-expected ratio is 1.68. For each game g define $z_g = (N_{\text{obs}}(g) - E_g) / \sqrt{V_g}$, the number of noise-null standard deviations by which the observed reversal count $N_{\text{obs}}(g)$ exceeds its null expectation. The mean of z_g across the 50 benchmark games is +3.2 and the median is +0.97. Thirty percent of games have $z_g \geq 2$, and thirty-four percent have $z_g \leq 0$. The right tail is what drives the average. A substantial subset of the benchmark games carries significantly more per-game disagreement than sampling noise can produce, while another sizeable subset is consistent with the noise null.

To assess whether significant parts of the game space carry reversals beyond what sampling noise alone can produce, we apply the Benjamini–Hochberg procedure to the one-sided excess-reversal p -values $\hat{p}_g = 1 - \Phi(z_g)$ across the 50 benchmark games. At a false-discovery rate of $q = 0.05$, **15 of 50 games** (30%) carry statistically more rank reversals than the noise-only null predicts. At $q = 0.10$, **19 of 50 games** (38%) do. Under the null that no game in the benchmark has any per-game variation beyond sampling noise, the expected number of false positives at $q = 0.05$ is at most 2.5. The observed 15 therefore constitutes clear evidence of per-game variation beyond the noise null on a non-trivial slice of the benchmark.

At the finer per-(pair, game) level, we identify 311 candidate reversal cells (game seeds, model pairs where the per-game point estimate reverses the overall leaderboard). For each candidate cell we compute a one-sided bootstrap p -value (fraction of bootstrap replicates in which the reversal does not hold). After BH-FDR correction across the 311 candidates, **five individual reversal cells survive** $q < 0.05$ and ten survive $q < 0.10$. The five $q < 0.05$ cells are: seed 2385 where gemini-3.1-flash-lite outperforms gemma-4-31b; seed 3483 where claude-sonnet-4-6 outperforms gemini-3.1-pro; seed 6635 where deepseek-v3.1 outperforms gemma-4-31b; and seeds 8297 and 10137 where gemma-4-31b outperforms gemini-2.5-pro. These are mid-pack rearrangements rather than upsets of the top three by the bottom of the table.

Reversal significance across axis space. Figure 8 plots the 50 benchmark games in the canonical state-space versus information-sensitivity plane, with each point coloured by its BH-FDR q -value on the excess-reversal test and the marker shape distinguishing the three significance bands. On no single axis taken alone do the reversal-significant games cluster cleanly into one tertile, and q -values vary across the full observed range of each axis.

Reversal significance by composite-complexity tertile. The composite-complexity score (PC1 of the per-model slope matrix; see Appendix I) combines the six axes into a single per-game difficulty proxy. Cross-tabulating the rank-reversal test against the composite-complexity tertiles shows that reversal significance is concentrated almost entirely on the easiest tertile.

Tertile	n	$q < 0.05$	$q < 0.10$	mean obs	mean exp	mean z
T1 (easiest)	16	12	14	9.19	1.76	+9.03
T2 (mid)	17	3	4	5.12	3.74	+1.35
T3 (hardest)	17	0	1	4.53	5.50	-0.40

The mean obs column is the average per-game count of observed pairwise rank reversals within the tertile, and mean exp is the average per-game count expected under the noise-only null defined above. The mean- z column reports the per-tertile average of z_g , the number of noise-null standard deviations by which the observed reversal count exceeds its null expectation.

Twelve of the sixteen easiest games carry BH-significant excess reversals at $q < 0.05$, with a mean z -score of +9. The seventeen hardest games have zero BH-significant reversals and a mean z close to zero. On hard games, the top models pull away from the rest with larger absolute margins (Section 6),

⁹Treating the 36 per-pair reversal indicators as independent Bernoullis gives the Poisson-binomial expectation E_g and variance V_g ; we use the standard-normal approximation to z_g for the one-sided p -value $\hat{p}_g = 1 - \Phi(z_g)$. The independence assumption is not strict, since the per-game $\hat{\alpha}_{m,g}$ for different models share information through the joint per-game refit, but this is the standard construction for a sum of correlated Bernoulli indicators.

so the rank ordering is stable and matches the overall leaderboard. On easy games the absolute gaps are small, and the per-game ranking reorders the field beyond what the per-pair sampling noise alone can produce. The per-game capability variation we surface in this appendix exceeds the noise null but is concentrated on easy games. Hard games are where the overall leaderboard is most trustworthy, and easy games are where it most under-represents per-game disagreement.

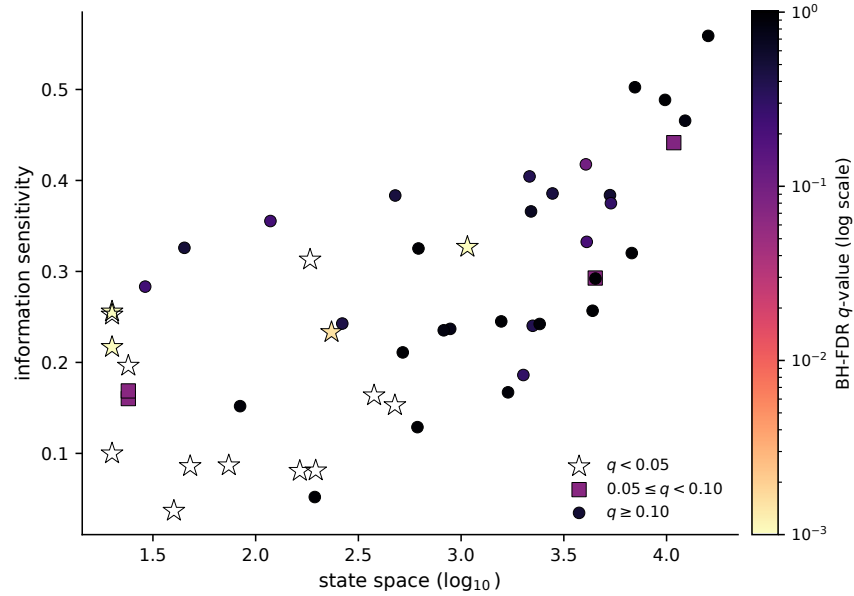


Figure 8: **Reversal significance in axis space.** The 50 benchmark games plotted in the state-space versus information-sensitivity plane (matching Figure 1), colour-coded by BH-FDR q -value on the one-sided excess-reversal test. Stars mark games with $q < 0.05$, indicating per-game rank reversals that are statistically significant at FDR 5% after correcting across the 50 games. Squares mark games with $0.05 \leq q < 0.10$ (marginal significance). Circles mark games with $q \geq 0.10$ (consistent with the noise null).